SANDIA REPORT
SAND2021-14967
Printed November 2021

Sandia National Laboratories

Deployable Wind-Hybrid Power Systems for Defense and Disaster Response Applications

Brian Naughton

Prepared by
Sandia National Laboratories
Albuquerque, New Mexico
87185 and Livermore,
California 94550

Issued by Sandia National Laboratories, operated for the United States Department of Energy by National Technology & Engineering Solutions of Sandia, LLC.

Available to DOE and DOE contractors from
U.S. Department of Energy
Office of Scientific and Technical Information
P.O. Box 62
Oak Ridge, TN 37831

Telephone: (865) 576-8401
Facsimile: (865) 576-5728
E-Mail: reports@osti.gov
Online ordering: http://www.osti.gov/scitech

Available to the public from
U.S. Department of Commerce
National Technical Information Service
5301 Shawnee Rd
Alexandria, VA 22312

Telephone: (800) 553-6847
Facsimile: (703) 605-6900
E-Mail: orders@ntis.gov
Online order: https://classic.ntis.gov/help/order-methods/

ABSTRACT

This report presents an analysis of the performance of deployable energy systems comprised of wind energy systems integrated with diesel generators, photovoltaic systems, and battery storage to meet the load requirements of a representative U.S. Army forward operating base. The analysis is conducted using HOMER, a microgrid analysis software that can search through a wide range of parameters to design and optimize microgrid power systems. The search parameters include the system architecture, the wind and solar resources, and the availability of diesel fuel. The results of the analysis measure the relative performance of the different systems and environments in terms of the overall transportation cost to deploy the system and the ability to provide resilience in terms of meeting mission critical loads.

ACKNOWLEDGEMENTS

The author would like to thank the following individuals for their support, feedback and review to improve this report: U.S. Department of Energy Wind Energy Technologies Office, Patrick Gilman and Bret Barker; Idaho National Laboratory, Jake Gentle and Dylan Reen; The National Renewable Energy Laboratory, Brent Summerville and Tony Jimenez; University of Dayton Research Institute, Eric Lang. In addition, numerous discussions with military and industry stakeholders over the past three years were invaluable in focusing the efforts represented in this report.

CONTENTS

1. Motivation and Approach 15
   1.1. Background 15
   1.2. Study Objectives 15
   1.3. Analysis methods 16
2. Modeling Assumptions and Input Parameters 17
   2.1. Contingency Base Reference System 17
      2.1.1. Background 17
      2.1.2. FCIL Power System 18
      2.1.3. Logistics Equipment 21
   2.2. Electrical Generation Device Models and Assumptions 22
      2.2.1. Diesel Generators 22
      2.2.2. Wind Energy System Models 22
         2.2.2.1. Three-bladed, Tower-Mounted D3T Wind Turbine Model 23
         2.2.2.2. Airborne Wind Energy System with Tether and Ground-Mounted Generator 24
      2.2.3. Solar Photovoltaic Model 26
      2.2.4. Battery Storage and Converter Model 27
      2.2.5. Microgrid Controller 28
   2.3. Resource Models 29
      2.3.1. Wind Resource Models 29
      2.3.2. Solar Resource Models 31
      2.3.3. Diesel Resource Models 32
   2.4. General Model Parameters, Assumptions and Constraints 33
   2.5. Assessment Metrics 34
      2.5.1. Transportation Burden Metric 34
      2.5.2. Footprint Metric 35
      2.5.3. Resilience Metric 36
3. Modeling Results 37
   3.1. Parametric Analysis of Transportation Optimized Microgrids 37
      3.1.1. Simple Payback Analysis 37
      3.1.2. Transportation Optimized Microgrids Results 38
      3.1.3. Summary 45
   3.2. Seasonality and Complementarity Analysis Results 46
      3.2.1. Diurnal Complementarity 46
      3.2.2. Seasonal Complementarity 47
      3.2.3. Summary 48
   3.3. Mission Resilience Results 48
      3.3.1. Constrained Diesel Fuel and Unmet Loads 49
      3.3.2. Mission Critical Loads 51
      3.3.3. Summary 53
   3.4. Airborne Wind Results 53
      3.4.1. Simple Payback Analysis 53
      3.4.2. HOMER Transportation-Optimized Systems 53
      3.4.3. Summary 55
4. Conclusions 57

References 59
Appendix A. Full Results from Seasonality Analysis 61
Appendix B. Resilience Scenario Results 64
Appendix C. Critical Load Analysis 67
Distribution 68

LIST OF FIGURES

Figure 1. Rendering of various deployable wind and solar power concepts at a forward operating base. Courtesy Besiki Kazaishvili, National Renewable Energy Laboratory....15
Figure 2. Future Capabilities Integration Lab at Fort Devens, Massachusetts represents two 150-solider Force Provider Expeditionary basecamp systems developed by the US Army....18
Figure 3. Future Capabilities Integration Laboratory electrical one-line diagram....19
Figure 4. Summer and winter daily load profiles for the FCIL....20
Figure 5. Fuel consumption for the AMMPS 60-kW generators....22
Figure 6. Conceptual rendering (L) and power curve (R) for the hypothetical D3T 3-bladed tower-mounted wind turbine model....24
Figure 7. Global average wind speed as a function of land surface area and height above ground. Data from the Global Wind Atlas [5]....25
Figure 8. Conceptual crating for the deployable PV system into a 462L pallet, two of which occupy the same logistical footprint as a single 20-ft shipping container. Rendering courtesy of the University of Dayton Research Institute....26
Figure 9. Distribution of measured wind speed diurnal strength parameters collected from measurement stations across the U.S. over multiple years....30
Figure 10. Daily solar radiation and clearness index by month for an equatorial location in Gabon....32
Figure 11. Daily solar radiation and clearness index by month for a location in Croatia near 45 °N latitude....32
Figure 12. Transportation optimized microgrid architecture in low solar resource. Diesel generator only system is the maroon area, diesel plus PV in pink, and diesel, PV and wind in green....38
Figure 13. Transportation optimized microgrid architecture in high solar resource. Diesel generator only system is the maroon area, diesel plus PV in pink, and diesel, PV and wind in green....39
Figure 14. Transportation burden of different combinations of wind turbines and PV systems in a low solar and wind resource scenario for 1, 3, 6, and 12 months....41
Figure 15. Transportation burden of different combinations of wind turbines and PV systems in a high solar and wind resource scenario for 1, 3, 6, and 12 months....42
Figure 16. The quantity of 6T Li-Ion batteries deployed for each combination of wind and PV systems for 6 or 12 month durations at low wind and solar and high wind and solar resources. The color of the lines corresponds to the number of PV systems deployed with red indicating zero PV and purple a higher number as indicated with each dot along a single color representing an increasing number of wind turbine systems from left to right....44
Figure 17. For each of the wind and solar resource combinations, the sensitivity of the number of batteries to the transportation burden is shown with the optimum number of 6T batteries in green text and the low and high extremes in blue....45
Figure 18. Percent unmet load for various levels of available diesel fuel and resource scenarios for a system architecture of 6 PV systems, 6 wind systems, and 4 battery containers....50
Figure 20. Percent unmet load for various levels of available diesel fuel and resource scenarios for a system architecture of 12 PV systems, 0 wind systems, and 4 battery containers....50
Figure 19. Percent unmet load for various levels of available diesel fuel and resource scenarios for a system architecture of 0 PV systems, 12 wind systems, and 4 battery containers....50
Figure 21. Daily load profile for the top four critical loads at the FCIL base model, representing about 22% of the overall base loads....51

Figure 22. Transportation-optimized microgrid architectures in a low (top) and high (bottom) solar resource. Red is diesel plus battery, orange is diesel, battery plus airborne wind, and green is diesel, battery, airborne wind and PV. The diamonds represent the total truck trips necessary to deploy each system 54
Figure 23. Percent unmet load (diamonds) for various levels of diesel fuel availability for a system architecture consisting of 6 wind systems, 6 PV systems, and 4 battery storage containers 64
Figure 24. Percent unmet load (diamonds) for various levels of diesel fuel availability for a system architecture consisting of 12 wind systems, 0 PV systems, and 4 battery storage containers 65
Figure 25. Percent unmet load (diamonds) for various levels of diesel fuel availability for a system architecture consisting of 0 wind systems, 12 PV systems, and 4 battery storage containers 66

LIST OF TABLES

Table 1. FCIL individual circuit average loads in winter and critical load priority 20
Table 2. Wind turbine specifications for 20-ft container 23
Table 3. Airborne wind system model parameters 26
Table 4. Deployable photovoltaic system model parameters 27
Table 5. Battery storage model parameters 28
Table 6. Wind resource parameters defining the low and high scenarios 29
Table 7. Solar resource parameters 31
Table 8. HOMER simulation optimization variables and fixed parameters 33
Table 9. HOMER simulation sensitivity variables 33
Table 10. Transportation equivalents for power system components 34
Table 11. Capital cost values used in HOMER to represent transportation burden 35
Table 12. Footprints requirements for each component 35
Table 13. Transportation optimized system architectures for different wind and solar resource complementarities. 47
Table 14. Summary of the seasonality and diurnal solar and wind resource complementarity variation on 1-month mission duration fuel and transportation burden 48
Table 15. Mission resilience system architectures 49
Table 16. Transportation-optimized systems that meet critical loads without diesel fuel. 51
Table 17. Transportation payback for the critical load renewable system in low and high resource. ..52
Table 18. Comparative 1-year performance of the different renewable generator models. 55
Table 19. Seasonality analysis for 1-month and 3-month missions with wind and solar resource peak both occurring at 12 pm 61
Table 20. Seasonality analysis for 1-month and 3-month missions with wind and solar resource peaks at 6 pm and 12 pm respectively 62
Table 21. Seasonality analysis for 1-month and 3-month missions with wind and solar resource peaks at 12 am and 12 pm respectively 63
Table 22. Optimal system architectures to meet critical base loads without diesel 67
Table 23. Critical load optimized architectures with full load and unlimited diesel fuel 67
Table 24. Optimal architectures without constraints on amount of renewables or diesel 67

This page left blank

EXECUTIVE SUMMARY

Rapidly deployable power systems are a critical element of every response to conflict and natural disasters globally. Much like power generation around the world in general, rapidly deployable energy systems largely depend on fossil fuel resources through a complex and often fragile supply chain that presents significant risk to mission success. The U.S. military has identified the need for energy alternatives in their strategic planning and investments to address such supply chain risks. Much of the focus on fossil fuel alternatives thus far has focused on solar photovoltaics with very little consideration for the potential value of energy from deployable wind turbines. Building off a prior study [1] that considered the technical characteristics that would improve the performance of deployable wind on its own, the present study expands the view to include solar photovoltaic systems and battery storage to consider integrated hybrid system benefits.

The analysis in this report relied primarily upon the Hybrid Optimization of Multiple Energy Resources (HOMER) microgrid simulation tool to explore a wide range of system parameters and to optimize systems for mission-relevant metrics like transportation burden and mission resilience. The analysis focused on a single reference system that was modeled on the Future Capabilities Integration Laboratory (FCIL), a U.S. Army research base and laboratory with a mission to evaluate new energy generation technologies, among many other objectives. The FCIL reference system provides detailed real-world electrical loads, including critical loads, to support the modeling accuracy and real-world relevance. The investigated system characteristics included a wide range of both system architectures and energy resource scenarios. This was done both to represent the wide range of environments globally where wind and solar resources vary considerably, and also to highlight general trends in wind-hybrid power system performance that can be broadly applied to any particular location or mission.

Four sets of scenarios were explored in this report.

The first set of scenarios varied multiple parameters including the system architecture, the wind resource, the solar resource, and the mission duration to assess the impacts on the overall transportation burden of the power system. For these scenarios, an equatorial location was used as the reference location because the solar resource remains fairly constant year-round. This was chosen so that the solar and wind resource remained at their respective average values regardless of how long the mission duration lasted.

The second set of scenarios considered the impacts of mission duration and time of year on the hybrid system performance. In this set of scenarios, the solar resource was varied throughout the year by selecting a location near 45 °N latitude, creating a significant difference in summer and winter performance. The objective of these scenarios was to understand how wind and solar resources can complement each other to better match load, both in daily and seasonal time cycles.

The third set of scenarios considers a situation where the supply of diesel fuel to the base is limited or interrupted to varying degrees. Scenarios include the impacts of limited fuel supply on the percent of unmet load given different resources and architectures and the renewable system design required to meet 100% of the critical loads of the base.

For the fourth set of scenarios, a model of a deployable airborne wind energy system was included along with the wind and photovoltaic system models used in the other scenarios. The model was adapted from a near-commercial airborne wind system. The airborne system is designed to operate high above the ground where wind speeds are typically much greater and more consistent than those closer to the ground, thus providing a significant potential performance benefit.

As a result of the modeling and simulation scenarios explored in this study, the following general observations provide some guidance as to where deployable wind systems can provide unique value.

The average wind resource varies widely across the world, and even within a single location through the day or year. The available power in the wind scales with the cube of the wind speed, so a doubling of wind speed increases the power by 8-fold. This nonlinear characteristic of wind energy means that wind systems perform significantly better in higher wind resources than in low resources. Photovoltaic systems don't generally have such drastic performance variability except in higher latitudes where seasonally they can vary significantly, for instance summer to winter.

Hybrid wind-PV systems generally outperform either just wind or just PV systems. Wind energy can be a valuable complement to a PV system depending on the load profile and resource characteristics. If there is a significant load at night, a PV-only system will require more panels and more batteries to meet that load. The addition of some amount of wind energy to that system could produce some power at night, especially where a strong evening or nighttime diurnal peak occurs. Seasonally, a wind turbine may also provide significant value. In higher northern latitudes in the winter months, solar production is significantly lower than the average and wind provides a complementary generation.

When considering mission resilience, wind systems are a valuable complement to PV systems. When diesel fuel is easily accessible, it takes a longer time for a wind system to pay for itself in terms of a transportation cost, especially in a lower wind resource location. However, when diesel availability becomes irregular or unavailable, even in a low wind location, adding a wind system to a PV-battery system is more valuable than merely increasing the capacity of the PV-battery system due to the nighttime wind power production.

Airborne wind energy systems show a lot of promise especially in deployable applications. Modeling results indicate that airborne wind systems have quicker transportation burden payback times as compared to both traditional wind and PV and produce up to 3.7 times as much energy as a traditional wind turbine given a similar transportation burden. The results for the airborne wind model are impressive, but the technology is the most immature of the three technologies considered and extensive independent field-testing verification should be conducted to build confidence in the potential of airborne wind for deployable applications.

With these general conclusions regarding the potential value of deployable wind to mission needs, the recommended next step is to create opportunities to demonstrate deployable wind technologies in a relevant field environment to help validate performance and identify specific areas where additional improvements may be needed. Locations like the FCIL that have an existing microgrid that a deployable wind system could be integrated into would be particularly useful as many of the benefits arise from these hybrid power systems and such facilities are not yet common. Hands-on end-user experience and feedback would be an important element to incorporate into field demonstrations as these deployable systems must be successfully installed and operated with minimal training.

ACRONYMS AND DEFINITIONS

Abbreviation	Definition
ABL	atmospheric boundary layer
AC	alternating current
AMMPS	advanced medium mobile power sources
DC	direct current
FCIL	Future Capabilities Integration Laboratory
FOB	Forward Operating Base
GHI	global horizontal irradiation
HEMTT	Heavy Expanded Mobility Tactical Truck
HOMER	Hybrid Optimization of Multiple Energy Resources
ISO	International Standards Organization
LHS	load handling system
NATO	North Atlantic Treaty Organization
NPC	net present cost
PLS	palletized loading system
PV	photovoltaic
RE	Renewable Energy
STC	Standard Test Conditions
SWRS	solid waste recycling system

This page left blank

1. MOTIVATION AND APPROACH

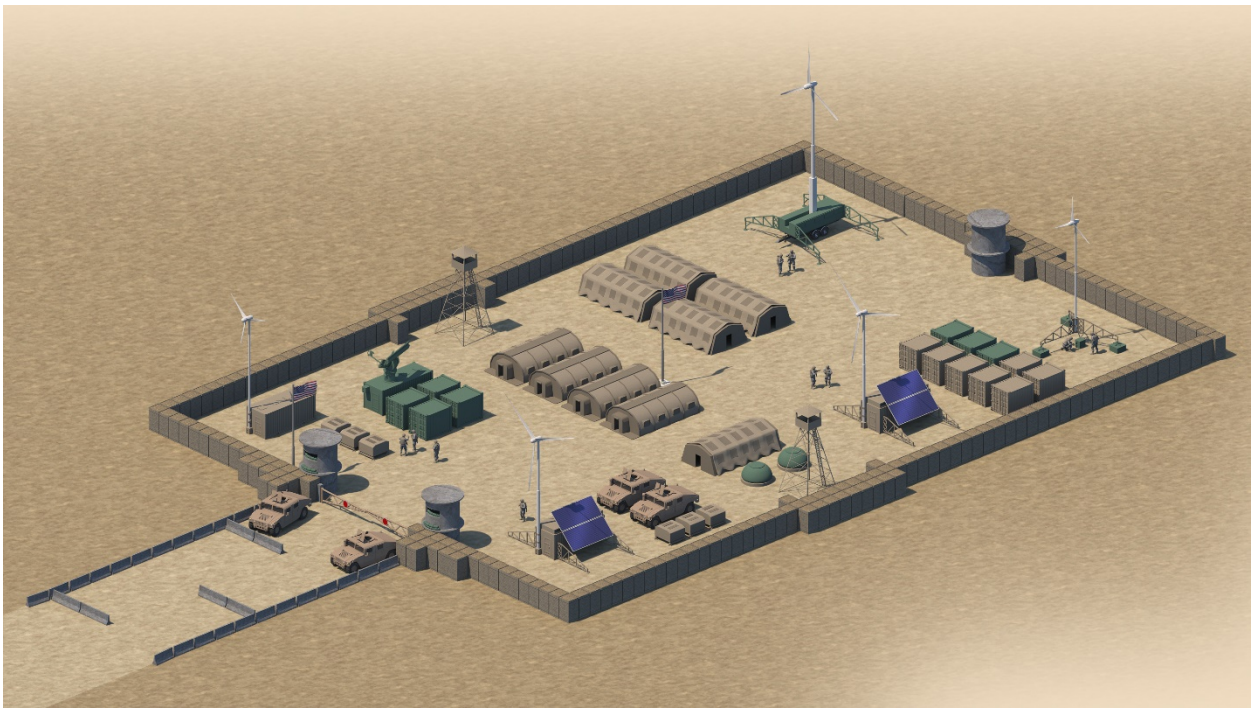

Figure 1. Rendering of various deployable wind and solar power concepts at a forward operating base. Courtesy Besiki Kazaishvili, National Renewable Energy Laboratory

1.1. Background

A prior study [1] investigated the potential benefits of wind energy provided by deployable wind turbines as quantified by a reduction in both fuel consumption and supply convoys to a hypothetical network of Army Infantry Brigade Combat Team bases. Two modeling and simulation tools were used to represent the bases and their operations and quantify the impacts of system design variables that included wind turbine technologies, battery storage, number of wind turbines, and wind resource quality. The combined results from both tools showed that wind turbines could provide significant benefits to contingency bases in terms of reduced fuel use (83% reduction) and number of fuel convoy trips (26% reduction) to resupply the bases. However, the prior analyses and subsequent discussions raised some additional questions regarding the role and potential value of deployable wind systems in defense and disaster response applications. As a result, this new study builds from the prior work to provide additional perspective and a more complete picture of the potential of deployable wind for defense and disaster response missions.

1.2. Study Objectives

Modeling and simulation analysis methods can provide useful insight into the potential value of a hypothetical deployable wind turbine operating in the context of a contingency base with different missions, located in different environments, and with a range of load profiles and generation mixes.

The three primary objectives of the current study are as follows:

1. Evaluate the performance differences of an isolated power grid (small forward operating base or 'FOB') with different mixes of distributed energy resources including diesel

generators, batteries, photovoltaic systems, and wind turbines, operating under different resource characteristics (wind, solar, and diesel availability).

2. Develop and compare performance metrics relevant to military mission profiles for the different scenarios, including diesel consumption, transportation burden, and time of unmet load.
3. Clarify the relative value of deployable wind systems under different system configurations and operating conditions to provide guidance to both planning and operational decision makers.

1.3. Analysis methods

The analysis for this report primarily relied on the Hybrid Optimization of Multiple Energy Resources (HOMER) Pro v3.13 simulation tool. HOMER is used for the design and optimization of microgrid power systems for a broad range of applications including military bases. HOMER has the capability to represent a wide range of generation types, energy resources, loads, microgrid controllers and optimization parameters for a single isolated microgrid power system. Models for the power system components are defined by the user including generation, loads, and controllers through a set of parameters that will be covered in a later section of this report. Resources including diesel, solar and wind are all defined as well. Finally, the optimization search space and constraints are also defined by the user. HOMER then iterates through a series of parameters the user has defined, for instance different system architectures or different wind and solar resources, using a series of energy balance time series simulations and then outputs the results for graphing and other analysis.

HOMER is designed to optimize systems using a single metric termed "net present cost." Net present cost is calculated by summing the present value of all the costs of installing and operating each component over the project lifetime, minus the present value of all the revenues that it earns over the project lifetime. These include capital costs, operating costs, replacement costs, fuel costs, and salvage value. HOMER attempts to minimize the net present cost of the system while also meeting the load, which in this analysis was generally 100% of the demand, though as will be discussed later, some scenarios were run where a percent of the load was allowed to be unmet for a resilience study. This type of economic analysis requires detailed knowledge of the component costs to arrive at a system that is properly optimized for minimum cost. This would make sense when designing a specific project, especially one where cost is a primary driver, but does not work well for the objectives of this current work.

Rather than optimizing systems for lowest cost, this analysis aims to optimize for alternative mission-centric metrics. One of the key metrics for power systems is to minimize transportation burden for a deployed system. Diesel generation at remote bases is a logistical burden because of the risks of transporting the fuel required to provide that power through contested territory. By calculating and optimizing for a power system that results in the lowest overall number of truck trips over the life of the base mission, components can be compared in a different and potentially more relevant way to mission objectives. Other metrics considered in this analysis are the overall physical footprint of the power system and also power system resilience which is defined by mission availability of uptime divided by the sum of uptime plus downtime [2].

2. MODELING ASSUMPTIONS AND INPUT PARAMETERS

This section provides the details, assumptions, and parameters used as inputs to the HOMER microgrid model. First, the selection and description of the baseline reference system is provided including the standard diesel power generation equipment and typical loads. Next, the assumptions and parameters for each of the power system device models is provided, including the diesel generators, wind and solar generation systems, battery storage, and microgrid dispatch controller. Next, the energy resource assumptions and parameters are defined, including the solar, wind, and diesel fuel availability. Finally, any additional general parameters, constraints and assumptions required for the HOMER model are provided along with the search space that was used for the simulations.

2.1. Contingency Base Reference System

The selection of a reference power system was driven by multiple factors. The first consideration was the relevance to DoD missions, so it was important to identify a standardized base unit that would be relatively common to the services. The second consideration was to find publicly available information that was sufficient to define the power system details to support the analysis. Finally, identifying a real-world facility that met the first two requirements was not strictly necessary, but was considered a potential benefit for future demonstration and testing capabilities to validate the modeling work. After reviewing a list of about a dozen potential reference systems, the U.S. Army's Future Capabilities Integration Laboratory (FCIL) was selected. The system represents a standard 150-person Force Provider Expeditionary basecamp, has detailed information on the power system including operational data that is public, and serves as a field experiment laboratory for testing new power system technologies among other objectives.

2.1.1. Background

The Future Capabilities Integration Laboratory (FCIL, Figure 2) is located at Fort Devens, MA and is operated by the U.S. Army to conduct experiments to evaluate technologies related to power, water, and waste to improve the operational efficiency of contingency bases. The camp covers four acres and represents the equipment and facilities of two identical 150-person Force Provider basecamps. Force Provider equipment is shipped in tricon shipping containers each weighing under 10,000 lbs. and includes billets, showers, latrines, and laundry, a kitchen, and support equipment. The Force Provider kit includes power generation and distribution, fuel support, water, and wastewater systems. The facility also serves as a training facility for soldiers who interact with the deployed systems in real-world scenarios.

The 150-person Force Provider systems are a standardized design that can be rapidly deployed and setup anywhere in the world, making it an ideal reference for this analysis. The Force Provider Operations field manual [3] defines the components, installation, and operation of the basecamp system. Some relevant details for the current analysis include:

- A single Force Provider 150-person module requires approximately 1 acre of land space and site preparation at a minimum
- Set-up time for each module is one to two days, from the time of breaking the seal of the containers to operational status
- The module requires a minimum of eight trained personnel with materiel handling equipment for set-up operations

- The Force Provider is intended to be set-up and in-place from 45 days to two years
- The fuel systems can store and distribute 1,200 gallons of diesel fuel using a tank and pump unit to refuel platoon equipment (1000 gallons just for the generators)

Figure 2. Future Capabilities Integration Lab at Fort Devens, Massachusetts represents two 150-solider Force Provider Expeditionary basecamp systems developed by the US Army

2.1.2. FCIL Power System

The power system for the FCIL is very well documented and defined. The electrical one-line diagram in Figure 3 shows the layout of the Six 60-kW Advanced Medium Mobile Power Source (AMMPS) mobile diesel generators connected in a microgrid configuration (AC bus) to the various circuits and end point loads. The primary loads for the base include:

- Two latrine systems
- Two shower systems
- One kitchen system
- One laundry system
- One refrigerated container
- Eight modular personnel tents (air supported) each with environmental control unit
- Two 400,000 British-thermal-unit water heaters
- One improved fuel distribution system

The FCIL has power meters on all of the major loads and collects data as part of the regular operations of the facility to support testing and analysis. The site operations manager provided two example daily loads for the base, one collected during a summer day and one during a winter day to represent the seasonal differences. The two daily load profiles are plotted in Figure 4. For all of the analysis conducted as part of this report, the winter load profile was used exclusively, simply because it is a larger overall load and more challenging to meet.

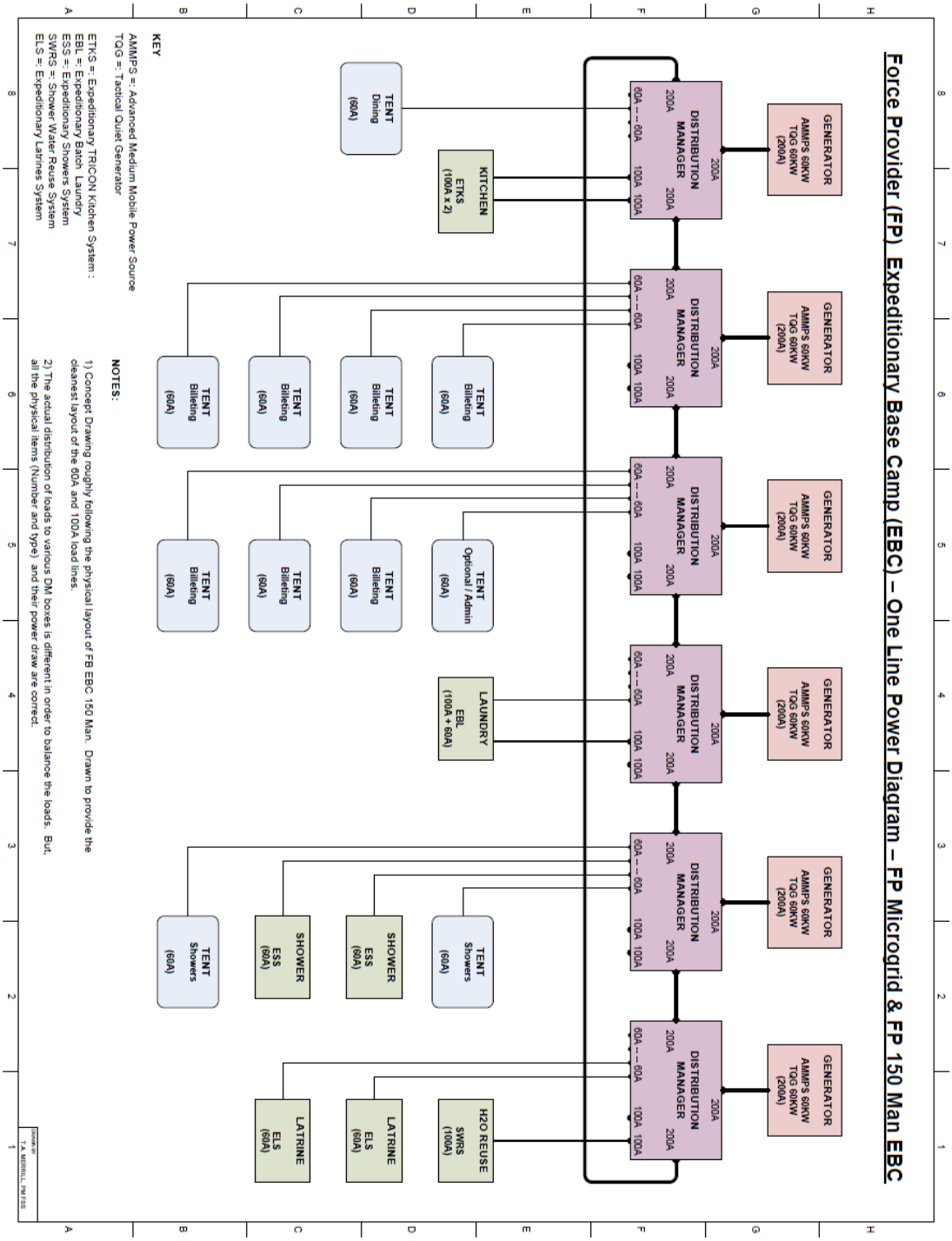

Figure 3. Future Capabilities Integration Laboratory electrical one-line diagram

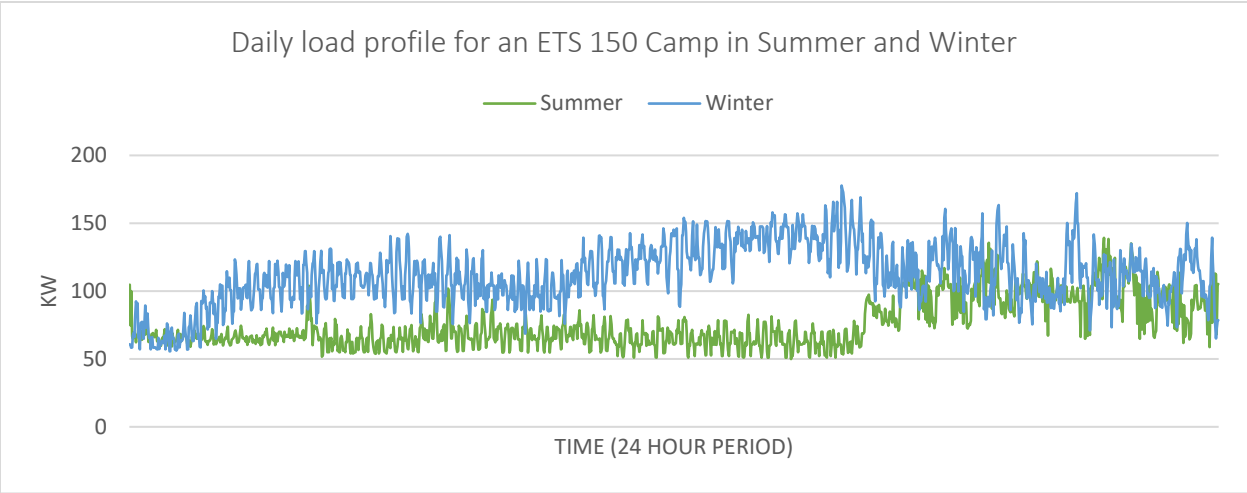

Figure 4. Summer and winter daily load profiles for the FCIL

The load profiles can be broken out by individual circuits that represent the major elements of the base. This level of detail is important for the resilience analysis that will be discussed later. The FCIL facilities manager provided the general critical load order for each of the circuits as shown in Table 1. The most critical load is that of the command tent, given priority 1. The least critical loads are given priority 5. The sum of the top four critical loads represents about 22% of the overall average loads for the entire base.

Table 1. FCIL individual circuit average loads in winter and critical load priority

Load	Average power - winter (kW)	Critical load order (1 = high, 5 = low)
Billeting		
Tent 25	7.535543	5
Tent 26	7.840352	5
Tent 27 (command tent)	5.951803	1
Tent 28	7.532389	5
Tent 29	7.293864	5
Tent 30	7.783773	5
Tent 31	7.73584	5
Tent 32	7.818848	5
Kitchen		
Container	1.095375	4

Load	Average power - winter (kW)	Critical load order (1 = high, 5 = low)
Container	4.397939	4
Tricold	0.719376	3
Tent	11.53528	4
Shower		
CTR Front	3.414358	5
CTR Back	3.4717	5
Tent Right	11.08472	5
Tent Left	8.387777	5
Latrine		
CTR 42	4.042013	5
CTR 47	0.783101	5
Laundry		
100 AMP	2.603209	5
60 AMP	2.628754	5
SWRS		
100 AMP	0.928101	2
Total	**114.5841**	

2.1.3. Logistics Equipment

The Force Provider Operations manual states that all of the equipment can be packed into tricon containers, each weighing no more than 10,000 pounds [3]. A tricon is a shipping container that can be connected to two other tricon containers to occupy the same footprint as a single 20-ft ISO shipping container. For the purposes of the analysis in this report, it is assumed that the deployed bases have access to Heavy Expanded Mobility Tactical Truck (HEMTT) equipment that is capable of handling up to 20-ft ISO shipping containers. The details of the HEMTT and container handling assumptions were covered in a prior report [1]. This assumption is important both for the footprint analysis as well as the logistics burden analysis that will be covered in a later section.

2.2. Electrical Generation Device Models and Assumptions

2.2.1. Diesel Generators

The FCIL and Force Provider basecamp standard package includes six 60-kW AMMPS generators. The generators are connected together as a microgrid in a ring configuration and thus are able to share loads. This microgrid configuration is not yet widely deployed, but DoD has indicated plans to do so and has developed a draft Tactical Microgrid Standard to provide the necessary technical requirements to facilitate the integration of multiple generation sources. For the purposes of this

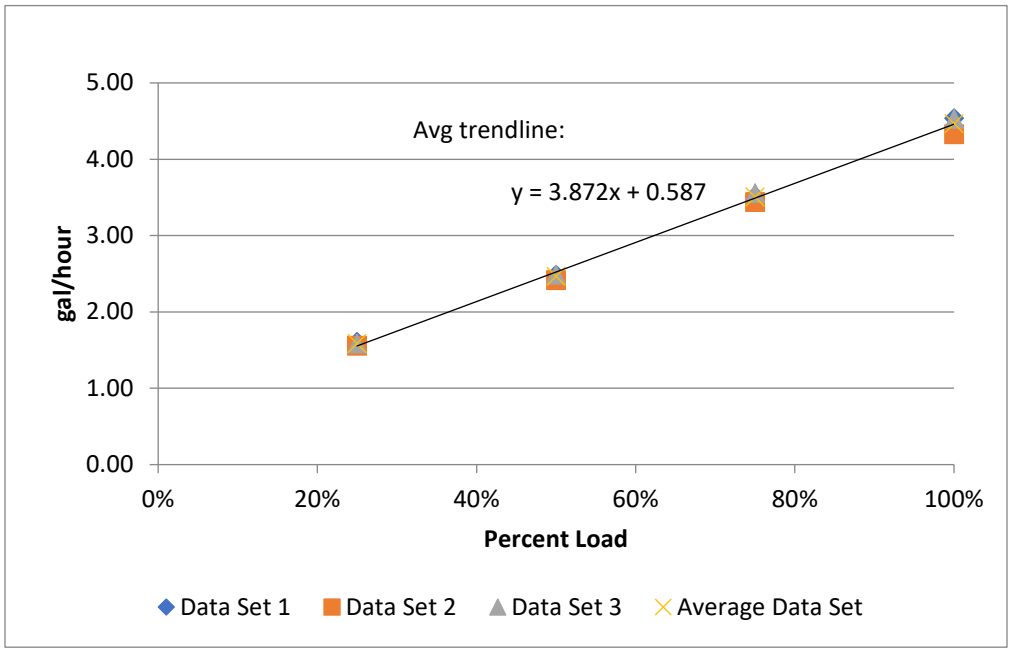

Figure 5. Fuel consumption for the AMMPS 60-kW generators

study, all power generation is assumed to be connected in a microgrid configuration. The US Army has determined through various studies that connecting diesel generators together on a single AC bus rather than acting as independent spot generators can reduce fuel consumption up to 30% [4]. The fuel consumption rate as a percent of output is provided in Figure 5.For all of the scenarios explored in this report, the baseline of six 60-kW AMMPS generators are included in addition to any of the other assets described in the following sections. Each 60-kW generator has dimensions of 82, 36, and 52.8 inches for the length, width, and height respectively and an overall weight for each unit of 3205 pounds [5]. With these parameters, it is assumed that four 60-kW AMMPS generators could be transported within a 20-ft ISO shipping container or equivalent given the dimensional and weight restrictions.

2.2.2. Wind Energy System Models

Two different wind energy system models were developed for this analysis, one is a more typical, 3-bladed, horizontal-axis wind turbine on a tower, and the second is a tethered airborne wind energy system with a ground-based generator. Most of the analyses incorporate the more typical 3-bladed wind turbine on a tower because the underlying technology is well-understood and has decades of commercial operation. The airborne wind energy system model is used for a single comparative analysis to evaluate the potential benefits of that technology compared to the traditional turbine

design. It is important to note that airborne wind is still an immature technology with almost no commercial deployments to this point so modeling results should be considered very preliminary until sufficient validation data is available.

2.2.2.1. Three-bladed, Tower-Mounted D3T Wind Turbine Model

For the purposes of this project, a hypothetical deployable wind turbine was designed to have the largest rotor and tower that could fit within the physical dimensions and weight restrictions of a 20-ft ISO shipping container. The design made use of hub extenders, which are cylindrical extensions connected between the central hub and each of the three blades. Hub extenders are used in some commercial wind turbine designs and add some additional swept area to the rotor to capture more energy. The largest single piece blade that could fit in the container is approximately 5.9 m (19.3 ft) but with the hub and hub extenders, the overall rotor diameter once assembled is 13.4 m (43.9 ft). The tower is a two-segment monopole design, with each section approximately 5.9 m (19.3 ft), same as the blades, leading to a fully erected hub-height of 11.7 m (38.5 ft). This is not necessarily the optimal design for a wind system, but it does provide an upper bound of the potential energy capture of a single wind turbine that would fit in the 20-ft shipping container. Additional technical details of the wind turbine model parameters are provided in Table 2.

Table 2. Wind turbine specifications for 20-ft container

Wind Turbine Design Parameter	Value
Coefficient of Performance (max)	0.40
Rated Power (kW)	25
Air density (kg/m3)	1.225
Blade length (m)	5.9
Rotor diameter (hub + blades) (m)	13.4
Rotor area (m^2)	140.6
Cut-in wind speed (m/s)	3
Rated wind speed (m/s)	8.4
Cut-out wind speed (m/s)	25
Specific power at rated (W/m^2)	177
Number of blades	3
Hub height (m)	11.7
System weight including container (kg)	6,400
Number of 20-ft containers required	1
System losses (%)	14
Deployed footprint (based on rotor diameter) (m^2)	140.6

Additional analysis was conducted on the wind turbine concept to ensure that the foundation was designed sufficiently to resist any overturning moments from both operational and extreme wind loads as documented in the deployable wind design guidelines report [6]. The final design required both outriggers and earth anchors for the selected rotor size as shown in Figure 6. If the rotor diameter is reduced from 13.4m to 11.85 m, then the earth anchors are no longer necessary.

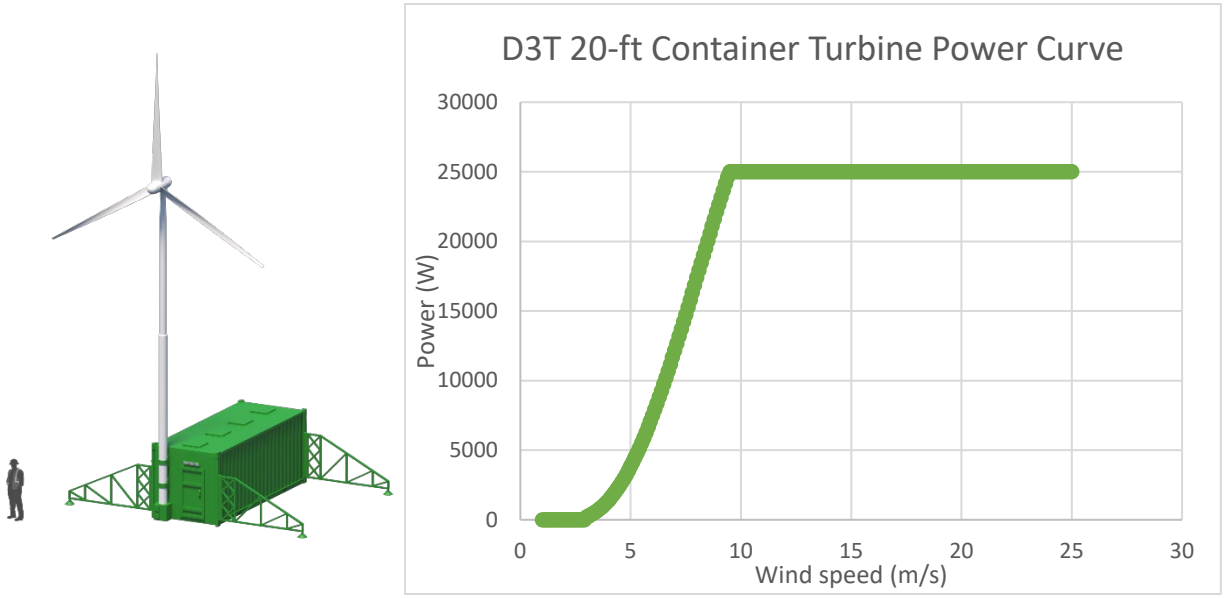

Figure 6. Conceptual rendering (L) and power curve (R) for the hypothetical D3T 3-bladed tower-mounted wind turbine model

The technical parameters in Table 2 were used to generate a power curve as shown in Figure 6. The HOMER model incorporates this power curve, along with the hub height and system loss factor of 14% to account for environmental factors, electrical losses, and downtime.

2.2.2.2. Airborne Wind Energy System with Tether and Ground-Mounted Generator

The second wind energy system model developed for this analysis is a generic representation of an airborne wind energy system that is connected to a ground-mounted generator via a structural tether. The basic design concept is that the soft or rigid kite reels out in the wind, pulling on the tether that is wound around a generator on the ground thus producing power. Then the kite must be reeled back in, consuming some power, but less than it produced, and the cycle repeats for a net positive power generation. The primary advantages of the airborne systems are 1) they can operate in relatively higher wind resources much further above the ground and 2) they need no tower that can be logistically difficult, especially for a rapidly deployable design.

The conceptual airborne model was adapted from an operational prototype airborne wind energy system with some technical details including a power curve provided by the prototype airborne wind energy company on the condition that the system is not publicly identified due to business needs. It is important to understand that while this information was based on experimental field data collected by the company, it has not yet been independently verified. Also, the airborne system has not yet been packaged into a deployable format that fits within 20-ft containers, however through

discussions with the company it appears viable that the system could be modified to fit within two 20-ft shipping containers. While it will be critical to verify and validate all of the modeled results of the airborne system performance, as well as the more traditional 3-bladed deployable turbines, it was deemed worthwhile to explore the potential benefits of the airborne design as an alternative concept that might warrant further research and development especially for the defense and disaster response applications.

The primary benefit of the airborne wind concept, as previously mentioned, is the access to better wind resources higher above the ground. Atmospheric physics is a complex subject, but it is generally the case that the atmospheric boundary layer (ABL) which represents the lowest part of the atmosphere in contact with the ground, generally displays a shear behavior in the wind speed due to the friction with vegetation and other elements of the ground surface. Thus, with increasing height off the ground, the wind speed increases for any particular location on the planet. Figure 7 shows the average wind speed at both 10 m and 200 m above ground as a function of the land surface area of the planet [7]. There is approximately a 4 m/s increase in average wind speed at the higher operational range of the airborne system. From a wind resource perspective, the available power in the wind scales with the cube of the wind speed, so a 4 m/s increase is very significant in terms of potential power production. This will be evident in the results presented later.

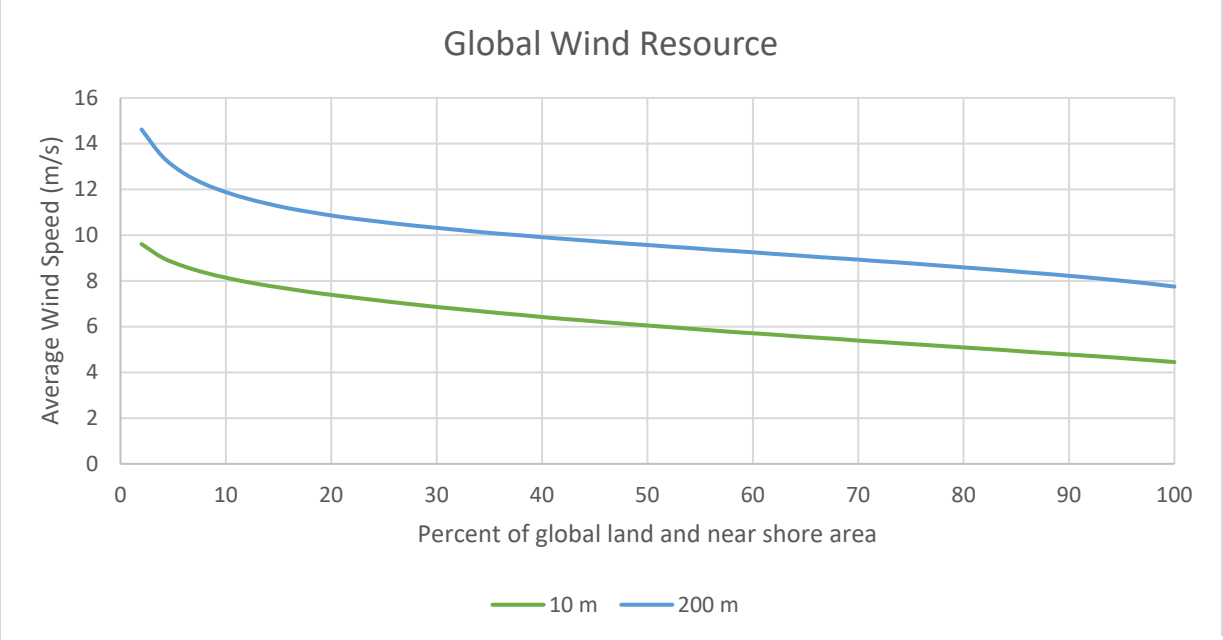

Figure 7. Global average wind speed as a function of land surface area and height above ground. Data from the Global Wind Atlas [5]

Though not published here by request, the airborne company did provide an experimentally derived power curve for the 100-kW rated system that was used in the HOMER analysis. This power curve incorporates and averages out all of the details of the actual operational cycle of the airborne wind energy system as it produces and then consumes power as it loops through its flight path. A 14% loss factor was applied to match the assumption used on the other wind turbine, though this could be quite different in practice and thus is another source of uncertainty. Unlike traditional tower-mounted turbines that are always deployed and generally able to immediate generate power as soon as the cut-in wind speed is achieved, the airborne system must return to the ground station and then redeploy when the minimum wind speed is not available. It is unknown how much this would

impact the availability of the system without additional long-term operational data. A summary of the technical parameters used in the HOMER model are provided in Table 3.

Table 3. Airborne wind system model parameters

Wind Turbine Parameter	Value
Rated power (kW)	100
Cut-in wind speed (m/s)	4
Rated wind speed (m/s)	13
Cut-out wind speed (m/s)	25
Number of 20-ft containers required	2
System losses (%)	14
Operational height (m)	>200
Deployed ground footprint (m^2)	27.5

2.2.3. Solar Photovoltaic Model

Unlike deployable wind turbine systems, solar photovoltaic (PV) deployable container systems are much more commercialized and readily available. A survey was conducted of nine different commercially available deployable PV systems that fit within a 20-ft shipping container. They were compared on metrics including overall weight, power output (DC), number of panels, overall footprint, and whether the system included power electronics and battery storage. The selected system was based on Armageddon Energy Rugged Panels which are a commercial PV product that is built upon a protective polymer sandwich panel that is much lighter than typical glass substrate panels. Each panel has its own microinverter. The system connects together quickly in a variety of configurations. The systems can be quickly deployed on the ground, on a conex, or a roof using a

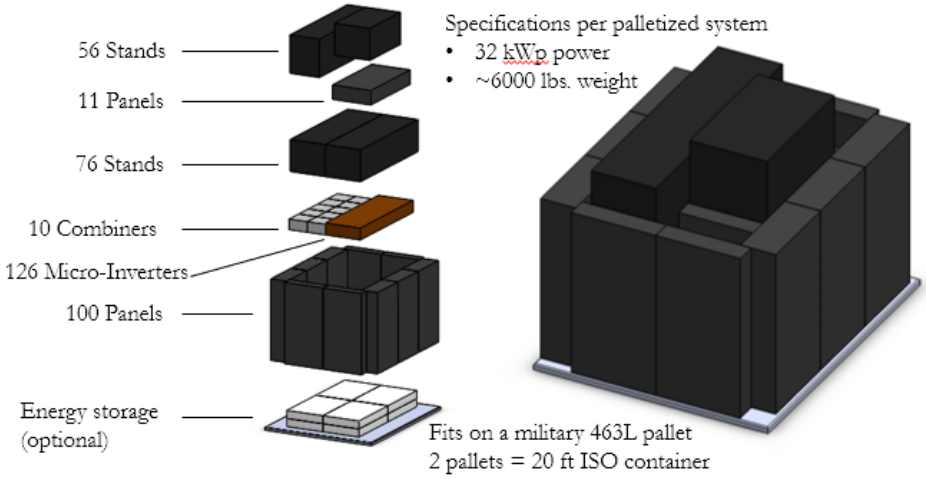

Figure 8. Conceptual crating for the deployable PV system into a 462L pallet, two of which occupy the same logistical footprint as a single 20-ft shipping container. Rendering courtesy of the University of Dayton Research Institute

ballasted mounting and rack system developed by a company called Sollega. A rendering of how the system could be palletized is shown in Figure 8.

The resulting system when sized to fit in a 20-ft shipping container has a rated DC power output of 64 kWp. As with the wind turbine, the system does not include integrated battery storage which will be discussed in the following section. The analysis assumes all the components connect to an AC microgrid, so the PV system does include the microinverters and there is an overall assumed system loss of 14% to cover the environmental, electrical, and availability losses. This loss is the same as used for the wind turbine models. Actual losses can be quite different for any deployable systems, especially environmental and availability losses, but those all depend on the specifics of the deployed environment and the operational methods of the power system. Table 4 summarizes the primary technical parameters used in the PV model. One additional assumption about the mounting system is that it can be designed to accommodate a range of tilt angles for the solar panels such that they can be optimally oriented to the sun depending on the time of year and latitude.

Table 4. Deployable photovoltaic system model parameters

Solar PV System Parameter	Value
Rated power (kWp DC)	64
PV panel rating (Wp DC)	280
Number of panels	220
Panel tilt angle	Variable, adjusted monthly to optimum angle to given latitude and time of year.
Number of 20-ft containers	1
System losses (%)	14
System weight (kg)	7,727
Deployed footprint (m^2)	375 (4,032 ft^2)

2.2.4. Battery Storage and Converter Model

A separate battery component was developed rather than have battery storage integrated into the individual generation components both because that is how it is represented in the HOMER simulation tool and because it then allows for optimizing the overall storage needs for the power system. In an actual deployed microgrid, it may be that the storage is either centralized or distributed across the power system or a mix of both. However, that is a design choice and detail that is beyond the scope of this analysis on bounding design cases rather than any particular power system.

Much like the deployable PV systems, there are also a variety of commercial battery storage systems that are containerized. Specifications on a range of commercial systems were compared to provide a sense of a realistic amount of battery storage that could fit into a 20-ft shipping container. It was found that even with the lighter-weight lithium-ion battery chemistry, weight was the driving factor for the system size. The lithium 6T battery format adopted by NATO as a battery standard was used for the battery technical specifications. The specifications were obtained from a product sheet provided by the company Epsilor and shown in Table 5 [8]. The details on the electrical integration

were ignored for this analysis because it is highly dependent on the design of an actual physical system and could be accomplished in a variety of ways depending on other design and operational objectives.

Table 5. Battery storage model parameters

Battery Parameter	Value
Nominal Voltage (V)	24
Nominal Capacity (kWh)	4.2
Nominal Capacity (Ah)	166
Roundtrip efficiency (%)	90
Maximum Charge Current (A)	130
Maximum Discharge Current (A)	260
Minimum State of Charge (%)	20
Weight (kg)	25
Maximum number of 6T batteries per 20-ft container	250

Due to the mix of DC (battery, PV) and AC (diesel generator, wind turbine) components on the power system, a generic, oversized power converter component was also included in the model. The power converter does not have any associated cost and has a conversion efficiency set at 95%. Typically, power converters are much smaller and lighter compared to the other system components and thus unlikely to contribute significantly to the transportation burden. Power converters are a critical part of a real power system design, but also require a level of analysis and detail that is beyond the scope of this work.

2.2.5. Microgrid Controller

The design of a microgrid controller for the management of generation and loads on the system would require its own separate detailed analysis. However, the HOMER tool does come with some default microgrid controllers that represent reasonably good approaches that could be optimized further for a more detailed system design. The two control approaches are termed Cycle Charging and Load Following.

The Cycle Charging strategy charges the battery using diesel generation, thus adding more energy to the battery, and making it more likely that the generator can be turned off in periods of low load. This strategy generally works best when the production from the renewables over the long-term (annually or seasonally) is less than the consumption or when there are just diesel generators and batteries on the system.

The Load Following strategy does not use the generator to charge the battery, rather this strategy leaves room in the battery to store excess renewable energy instead. The diesel generator is only used to power whatever load the renewable generators cannot meet at each time step. This strategy

generally works best when the production from the renewables over the long term (annually or seasonally) is greater than the consumption.

Both microgrid control approaches were simulated for each scenario to ensure the systems were operated optimally. More details can be found in the HOMER software manual [9].

The controller was also set to operate with the diesel generators always operating with a minimum loading depending on the amount of wind and solar energy being generated. This is termed "operating reserve" in HOMER and reflects the need for a reference AC voltage to be established by the diesel generators such that the inverter-based wind and solar generation systems can synchronize with that reference signal. The operating reserve was set at 10% of overall load, 50% of wind generation, and 80% of solar generation as default values in the HOMER tool. This ensures that there is sufficient spare power generation if the wind or solar resource suddenly drops or load suddenly increases. Some studies investigating the relative variability of wind and solar resources support the selected operating reserve values [10] [11]. There are inverter-based devices called grid forming inverters that could also provide the grid reference and enable the diesel generators to turn off completely and reduce the spinning reserve requirement for the wind and solar resources. This operating mode is considered in some scenarios with a very high percent of renewable energy backed up by sufficient battery storage. In these scenarios, a grid forming inverter coupled to a battery system would offer the backup power source to even out the intermittent renewable generation.

A best attempt was made in the present study to represent a reasonable but generic microgrid controller to support the simulations. The design and operation of a microgrid controller is a very large and complex topic that is important but beyond the scope of this report. There are various references available for more in-depth information on the current trends in microgrid control approaches for systems with renewable energy generators [12].

2.3. Resource Models

2.3.1. Wind Resource Models

As mentioned in Section 1.2, one of the objectives of this study is to explore the impacts of a range of energy resources on the operation of the reference base power system. In a prior study [1], the methods and reasoning were provided to define a "low" and "high" wind resource, based on global statistics and other considerations. The outcome was a set of technical parameters that were used to generate synthetic wind speed time-series within the HOMER tool as part of the simulation process. The same parameters were used again for this analysis as summarized in Table 6.

Table 6. Wind resource parameters defining the low and high scenarios

HOMER parameters	Low Wind Resource	High Wind Resource
Monthly average (m/s)	4.32	6.22
Weibull k	2.021	2.017
Weibull A	4.876	7.02
1-hour autocorrelation factor	0.85	0.85

HOMER parameters	Low Wind Resource	High Wind Resource
Diurnal pattern strength	0.25 (12 pm, 6 pm) 0.45 (12 am)	0.25 (12 pm, 6 pm) 0.45 (12 am)
Hour of peak wind speed	12 am, 12 pm, 6 pm	12 am, 12 pm, 6 pm
Altitude above sea level (m)	0	0
Anemometer height (m)	30	30
Surface Roughness	.01 (rough pasture)	.01
Wind speed shear scaling power law exponent	0.14	0.14

For this new analysis, the diurnal pattern strength was used as a variable rather than as a constant in the prior study. The timing and relative strength of the daily peak wind speeds were adjusted to happen at 12 pm, 6 pm, and 12 am. Additionally, for the 12 am diurnal peak, the strength was increased from 0.25 to 0.45, indicating that the increase of wind speed relative to the average was higher. The diurnal timing was selected to coincide with the solar resource peak (12 pm), to be maximally distant from the solar peak (12 am), and a time in-between those extremes (6pm). The strengths were chosen based on a statistical study of historical data from a few hundred measurement stations across the U.S. and summarized in the HOMER user manual [13]. The diurnal strength distribution in Figure 9 shows a big peak around 0.25 that is used for the standard case, and a second peak around 0.45 that is used in the 12 am case.

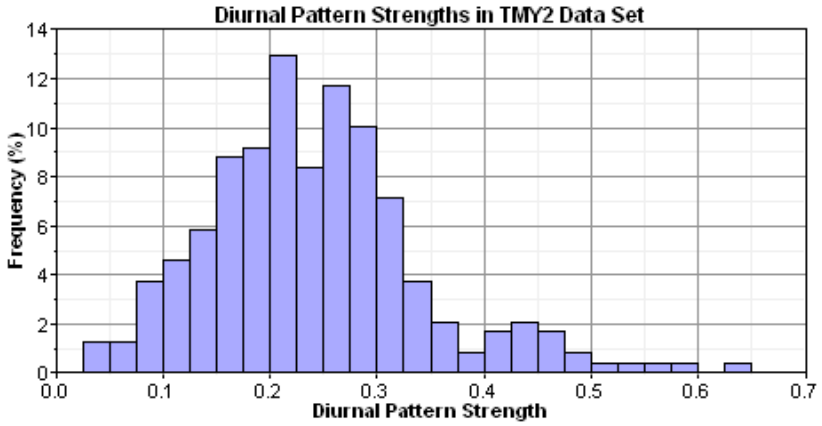

Figure 9. Distribution of measured wind speed diurnal strength parameters collected from measurement stations across the U.S. over multiple years.

As noted previously in Figure 7, the wind speed difference between the operational height of the 11.7 m high baseline turbine and the 200 m airborne wind energy system had to be defined in HOMER through a scaling parameter. A power law scaling was used and an exponent of 0.14 was found to reasonably match the plotted data.

2.3.2. *Solar Resource Models*

To mirror the wind resource model, a methodology was developed to arrive at a representative "low" and "high" average solar resource. The methodology started with global solar data which was obtained through the public Global Solar Atlas 2.0 website, a companion to the Global Wind Atlas, both efforts funded by the World Bank [14] [7]. The website provides a variety of solar resource data formats including global horizontal irradiation (GHI) expressed in units of kWh/m^2/day. GHI is based on a long-term average of the direct and diffuse irradiation but doesn't account for the PV system specifics or local specific environment like temperature, dust, wind, etc. The average GHI for each country was weighted by the country's land area to statistically define the "low" solar resource as that which occurs on 90% of the global land area and the "high" solar resource as that which occurs on the top 10% of global land area. This is similar to the approach used for the wind resource for the "low" resource definition. The reasoning for this approach is that defense and disaster response missions could theoretically happen anywhere on the planet and the resource may be unknown, so planning for the low resource, which at least 90% of the landmass has, is a good conservative reference. The "high" resources were used to demonstrate the upper end of what wind and solar systems could achieve. The low and high solar resources are provided in Table 7.

Table 7. Solar resource parameters

Global land area	Annual Average GHI (kWh/m^2/day)
10th percentile (high resource)	5.20
90th percentile (low resource)	4.21

Unlike the wind resource, HOMER does not synthetically generate solar resources based on a set of parameters. Instead, HOMER uses a physical location defined by latitude and longitude to pull from a database of historical data that are used to define a "typical year" of solar resource time series. Two different representative geographical locations were used for the simulations depending on the particular analysis objectives. For the more general, averaged, year-long scenarios, and also for the airborne scenarios, a location along the equator was chosen so that there was very little seasonal variation in the resource due to the consistent day length. The location was on the Atlantic coast of

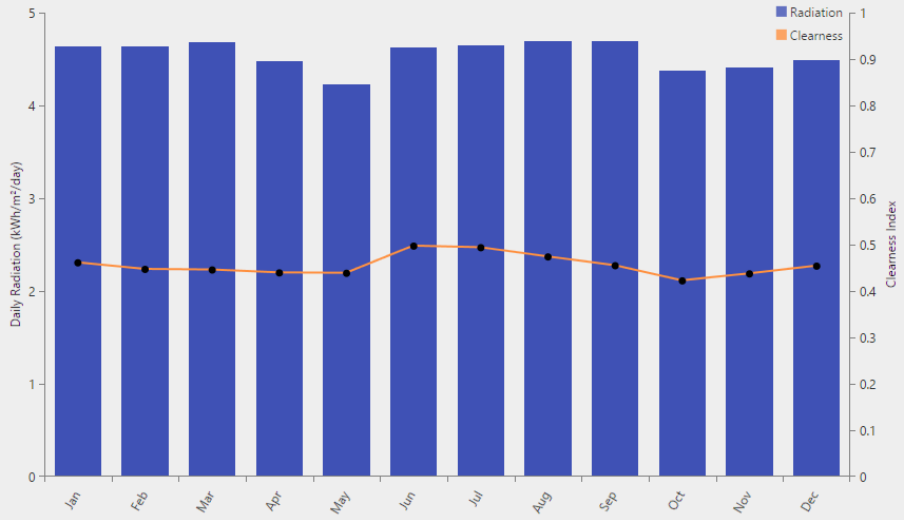

Gabon with a monthly solar radiation and clearness index as show in Figure 10 and within HOMER, the specific average value was scaled to the global high and low averages per Table 7.

For scenarios with durations shorter than a year, where seasonal variation in solar resource is an important factor, a location in Croatia near 45 °N latitude was chosen to emphasize the large variation from summer to winter. The GHI and clearness by month are shown in Figure 11.

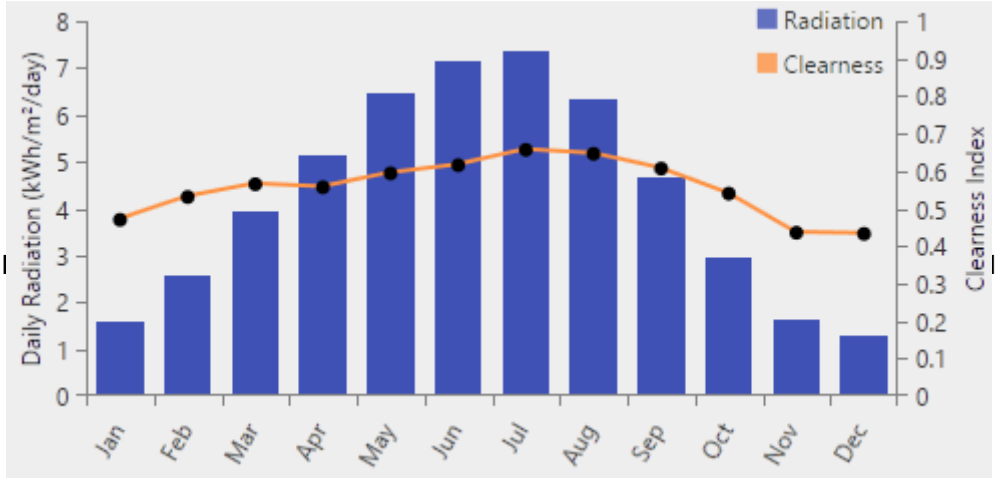

Figure 11. Daily solar radiation and clearness index by month for a location in Croatia near 45 °N latitude.

2.3.3. Diesel Resource Models

For most of the scenarios explored in this report the assumption was that diesel was resupplied without disruption as it was consumed. However, for the resiliency scenarios, the diesel fuel supply was restricted to various levels to assess the impact to the base in terms of meeting overall load and critical load with and without the addition of renewable energy generation and battery storage. At the highest end, 76,859 gallons of diesel was necessary to power the base for a year with just the diesel generators. With less diesel availability, either renewables had to make up the difference or loads were unmet, starting with the least critical loads.

From a transportation burden perspective, it was assumed that a single HEMTT fuel transport with a fuel trailer was capable of transporting 5,000 gallons of diesel in a single trip (2,500 gallons in the main fuel tanker and another 2,500 gallons in the fuel trailer). It was also assumed that there was the equivalent of 5,000 gallons of fuel storage available at the base, enough to supply the generators to meet the load for over 23 days. The U.S. Army issued Directive 2020-03, Installation Energy and Water Resilience Policy, establishing a requirement that critical missions be able to withstand a 14-day utility outage for energy and water. While this directive is aimed more at the permanent installations, it's a relevant goal for the contingency bases as well.

2.4. General Model Parameters, Assumptions and Constraints

In addition to the individual component and resource model definitions, HOMER also has general model parameters to be defined prior to running the simulations. These parameters include some general financial data, operational constraints, environmental considerations and also the details of how the simulations are conducted through optimization and sensitivity variables.

In general, the financial details of the project were not of interest for this analysis, so the values for the discount rate and interest rate were both set to 0. Environmental details like the impact of temperature were neglected. These parameters would be important for assessing the performance and economic viability of a specific project that was being financed but not for this more general, comparative analysis in this report. Likewise, as mentioned in the component analysis sections, there were no operation and maintenance cost, nor replacement cost associated with any of the generation equipment. The reasoning behind this assumption is that these deployments are typically less than one year, and it is also assumed that PV and wind components likely have similar maintenance requirements as the diesel generators. If reliability statistics are available from operational equipment, a future analysis could include such factors.

The optimization variables, summarized in Table 8, define the search space that HOMER explored in trying to optimize a system. The variables can be explicitly defined like the number of wind and PV systems, or defined as a range with an upper and lower bound, as with the number of batteries. Other parameters such as the diesel generator and power converter are fixed across simulations. If explicit search space values are provided, HOMER will optimize every combination of those values. In this analysis, every system will have a fixed power converter and diesel generator, and then for each combination of wind and solar system values, the number of batteries will be optimized for lowest transportation burden (i.e., "truck trips").

Table 8. HOMER simulation optimization variables and fixed parameters

Optimization Variables	Values
Number of wind systems	1, 2, 3, 4, 5, 6, 7, 8, 9, 10, 11, 12
Number of PV systems	1, 2, 3, 4, 5, 6, 7, 8, 9, 10, 11, 12
Number of 6T batteries	0 – 835 (optimization range)
Power converter capacity (kW)	9,999,999 (fixed)
Diesel generator capacity (kW)	6 x 60 kW (fixed)

The second set of simulation variables that are specified in HOMER are for sensitivity analysis. In Table 9, input variables for the project lifetime, average wind speed, average solar GHI, and allowable capacity shortage are summarized. Project lifetimes ranged from 1 to 12 months to examine the impact of mission duration on the relative benefits of renewable systems compared to diesel. A range of wind and solar resources were defined to explore the broad range of conditions found across the vast majority of the global landmass. The capacity shortage and diesel fuel quantity variables were used only in the resilience analysis. In the other analyses annual capacity shortage was set to 0 and diesel fuel quantity was unconstrained.

Table 9. HOMER simulation sensitivity variables

Sensitivity Variable	Values
Project lifetime (months)	1, 2, 3, 4, 5, 6, 7, 8, 9, 10, 11, 12, 18, 24

Sensitivity Variable	Values
Average wind speed (m/s)	4.32, 4.80, 5.27, 5.75, 6.22
Average solar GHI (kWh/m^2/day)	4.21, 5.20
Annual capacity shortage (%)	0, 1, 5, 10, 20, 30, 40, 50
Diesel fuel quantity (gallons)	0, 2500, 5000, 7500, 10,000, 12,500, 15,000, 17,500, 20,000

2.5. Assessment Metrics

Two metrics were considered in the assessment of all microgrid architectures. The primary method to evaluate designs was a metric to measure and minimize the transportation burden of the power system equipment and fuel. A footprint metric was also developed to compare across the system designs, though it was not used explicitly for optimization. For the resilience analysis, an additional metric based on the percent of time the load was successfully met was used.

2.5.1. Transportation Burden Metric

As introduced in Section 1.3, HOMER optimizes systems using a single metric termed *net present cost* (NPC). This is a useful financial metric to facilitate comparisons between different architectures and scenarios when optimizing a particular system where detailed cost and other financial data are fairly well known. For this analysis however, the aim is to minimize transportation burden rather than cost. To accomplish this, the transportation burden for different components had to be established and then those had to be represented properly in the HOMER model. Transportation assumptions were established for the diesel generator, diesel fuel, wind turbines system, solar PV system, and batteries. The basic unit of transportation, a "truck trip," is based on the capacity of the appropriate HEMMT transport system. The M1120 LHS with trailer can transport two 2,500-gallon modular fuel systems for a total of 5,000 gallons of diesel fuel per truck trip. Likewise, the PLS M1075A1 truck and PLS M1076 trailer can each hold a single 20-foot ISO shipping container. Using those two reference points, the transportation metrics are described in Table 10.

Table 10. Transportation equivalents for power system components

Component	HEMMT with trailer "truck trips"
60 kW AMMPS generator	0.125
5000 gallons of diesel fuel	1.0
25-kW wind turbine system	0.5
100-kW airborne wind energy system	1.0
64-kW solar PV system	0.5
6T Li-ion battery	0.004

The transportation assumptions were then used to modify HOMER to optimize for lowest truck trips instead of lowest net present cost. To accomplish this, all costs were set to zero for each component, including capital cost, operations and maintenance costs, fuel costs, replacement costs, and salvage values. Then a specific value was entered for the fuel and the capital cost of each component based on the transportation requirements in Table 10. The capital cost values are straight-forward with the equivalent number of truck trips represented in dollars (i.e., 1 truck trip = $1.00 capital cost). The fuel cost is slightly more complicated because HOMER uses liters as the

volume unit of fuel and the cost is entered on a per liter basis. The cost per liter was calculated as 1 truck trip divided by 5,000 gallons (18,927 liters) or 0.00005285 $/L.

Table 11. Capital cost values used in HOMER to represent transportation burden

Component	HOMER Capital Cost Representation
60 kW AMMPS generator	$0.125
5000 gallons of diesel fuel	0.00005285 $/L
25-kW wind turbine system	$0.50
100-kW airborne wind energy system	$1.00
64-kW solar PV system	$0.50
6T Li-ion battery (4.2 kWh)	$0.004

By incorporating only these values for capital cost and fuel cost and with all other costs set to zero including any finance rates, etc., the HOMER tool will optimize to minimize the number of truck trips using net present cost as a proxy.

2.5.2. Footprint Metric

The physical footprint of the base and power system components were evaluated because it is more costly to secure a larger defensible space, and wind and solar energy systems occupy a larger area compared to diesel generators on a per kilowatt-hour generating basis. The basic 150-person Force Provider kit requires about 340 ft by 520 ft of space or 176,000 square feet (~4 acres) [3]. This is enough space for the diesel generators, billeting, kitchen, and other equipment needed to operate the base, but it does not consider the space that might be required for larger deployments of renewables. Footprint assumptions were developed for each component based on product specifications and some assumptions about placement and operational space. The footprint values summarized in Table 12 are based on the following assumptions:

- 20-foot ISO shipping container is based on the length and width of a standard container
- Four 60-kW AMMPS generators were assumed to fit in a single 20-foot ISO container, so a single generator is assumed to take up a fourth of the container footprint when deployed
- 2500 gallons of fuel is assumed to take up the equivalent of single 20-foot container space
- The 25-kW wind turbine occupies a space that is determined by the area needed for the turbine to be able to yaw (rotate about the tower) in 360 degrees, to avoid hitting any other objects as it aligns with the wind
- The 64-kW PV system is driven by the footprint of all 220 panels placed flat on the ground
- 125 6T batteries can fit within a single 20-ft container footprint

Table 12. Footprints requirements for each component

Component	Footprint (ft^2)
20-foot ISO shipping container	159
60 kW AMMPS generator	39
2500 gallons of diesel fuel	159

Component	Footprint (ft^2)
25-kW wind turbine system	1520
64-kW solar PV system	4032
125 6T Li-ion batteries	159

There are a few important caveats with this simple footprint metric. The wind turbine system footprint is the minimum area it requires to not physically strike another turbine that is placed next to it. Typically, wind turbines are spaced out multiple rotor diameter distances away from each other, so multiple units would reasonably occupy even more overall space than is indicated here. However, PV systems could be interspersed on the ground between the wind turbines making more efficient use of the overall footprint. Finally, batteries could be integrated directly into the containers for the PV or wind systems and might not contribute much to the footprint overall.

2.5.3. Resilience Metric

Resilience is defined in a variety of ways depending on the objective of the analysis, but for power systems it generally refers to the ability of a system to recover from a major disturbance. For the purposes of this specific analysis, the definition of resilience is adapted from a February, 2020 memo published by the Office of the Undersecretary of Defense Acquisition and Sustainment [2]. In that memo, the metric "mission availability" is defined as:

$$Mission\ Availability = Uptime\ /\ (Uptime + Downtime)$$

Uptime is the length of time the critical mission operation requires energy throughout the year, and downtime is the length of time the critical mission operation can tolerate before mission failure occurs. The HOMER model calculates an output metric of percent unmet load, and when compared to the critical load (priority 1 through 4) for the base as defined in Section 2.1.2 and Table 1, a metric analogous to Mission Availability can be assessed.

3. MODELING RESULTS

The modeling results are organized around four groupings of scenarios, each with slightly different input assumptions as will be described in each of the following sections. The first grouping of results looks at the transportation burden of systems with different architectures (diesel, wind, PV, batteries), different resources (wind and solar), and different mission durations (1 – 24 months) but all at the same time of year (an annual average).

The second grouping of results considers a fixed system architecture that is also deployed for different durations but under this group, the systems are deployed at different times of the year to consider the impacts of seasonality on system performance.

The third grouping of results covers the resilience performance of different system architectures operating with different wind and solar resources and also with different levels of restricted diesel availability.

The final set of results evaluates the relative performance of an airborne wind system compared to the standard wind turbine and PV system models used in the previous scenarios.

3.1. Parametric Analysis of Transportation Optimized Microgrids

The first set of scenarios varied multiple parameters including the system architecture, the wind and solar resource, and the mission duration to assess the impacts on the overall system transportation burden. For these scenarios, an equatorial point in Gabon was used as the reference location because the solar resource remains fairly constant year-round. This was chosen so that the solar and wind resource remained at their respective average values regardless of how long the mission duration lasted. In the next set of results in Section 3.2 the impacts of the seasonality will be considered, for example a 1-month mission in winter vs. summer.

3.1.1. Simple Payback Analysis

The following simple energy payback calculations are intended to provide a simple verification to compare with the HOMER results in the subsequent sections. A simplified performance model of the FCIL reference base model was used to calculate the load per day and the required amount of diesel consumed each day by the diesel generators to meet that load. That baseline amount of diesel and equivalent electrical power was then compared to the average electrical output of the wind turbine model and the solar PV model operating in low and high solar and wind resources. The number of operating days can then be calculated before the wind and solar systems are able to offset an equivalent amount of fuel from a transportation burden perspective. Since both the wind and solar systems are designed to be transported within a single 20-foot ISO shipping container, it was established in Section 2.3.3 that the equivalent amount of fuel from a transportation perspective is 2500 gallons. Assuming an average fuel efficiency of 11.5 kWh/gal for the 60-kW diesel generators, 2500 gallons of fuel would result in 28,750 kWh of electrical energy.

The deployable wind turbine model has a rated power of 25 kW at a wind speed of 9.5 m/s, which is quite high. At the low wind resource, defined as 4.32 m/s, the wind turbine output is only 2 kW. To produce as much energy as 2500 gallons of diesel (equivalent transportation burden) the wind turbine would require 28,750 kWh/2 kW = 14,375 hours or about 598 days of operation at low wind. At the higher wind resource, defined as 6.22 m/s, the wind turbine produces 8.5 kW of power. Using the same methodology, this would provide a payback of a much shorter 140 days.

The deployable PV system model has a Standard Test Conditions (STC) rated power of 64 kW. At the low solar resource, defined as 4.3 kWh/m^2/day, the PV system would produce at rated for the equivalent of 4.3 hours producing 275 kWh/day. At this production, the PV system would produce the equivalent amount of energy as 2500 gallons of diesel fuel in 28,750 kWh/275 kW/day = 104 days. At the high solar resource, defined at 5.2 kWh/m^2/day, the system produces 352 kWh/day. Using the same methodology, this system would pay for itself in only 82 days.

3.1.2. Transportation Optimized Microgrids Results

The first set of figures shows the general composition of the transportation optimized system architecture as a function of solar resource, wind resource, and deployment time. Figure 12 shows the optimum system architecture as a function of wind speed and deployment time in a low solar resource whereas Figure 13 shows the same but in a high solar resource. In both figures, systems with diesel generators only are represented by the maroon area, diesel and PV in pink, and diesel, PV, and wind in green.

In a low solar resource (Figure 12), the inclusion of PV starts to become optimal over more diesel starting at 5 months. In the high wind resource, the inclusion of wind turbines with PV and diesel also becomes optimal at that same 5-month point. In the low wind resource scenario, the addition of wind turbines does not become optimal until beyond 1 year. This correlates fairly well with the simple payback calculations.

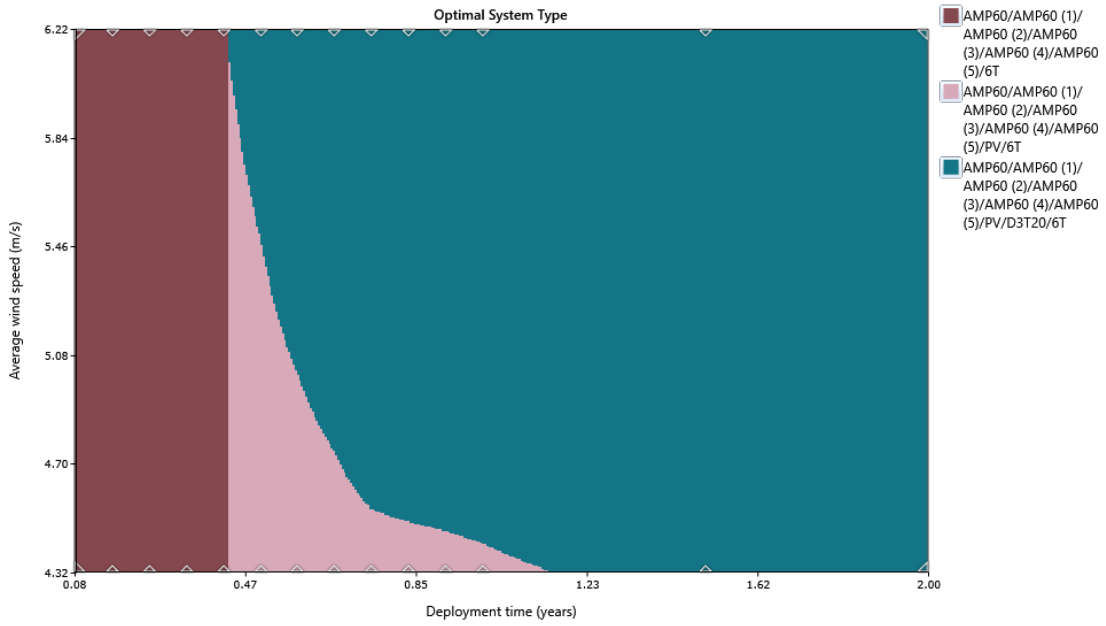

Figure 12. Transportation optimized microgrid architecture in low solar resource. Diesel generator only system is the maroon area, diesel plus PV in pink, and diesel, PV and wind in green.

In a high solar resource (Figure 13), the inclusion of PV becomes optimal over more diesel at around 4 months. In the high wind resource, the inclusion of wind turbines with PV and diesel becomes preferable between 5-6 months. In the low wind resource scenario, the addition of wind turbines does not become optimal until almost 2 years. This also correlates fairly well with the simple payback calculations presented earlier.

From a strictly transportation burden perspective, it's only beneficial to incorporate renewables into a system if the mission duration is longer than about 4 months. However, this analysis does not

consider seasonal variability in wind and solar resources that could be either higher or lower than what was analyzed here. This question is covered in more detail in Section 3.2.

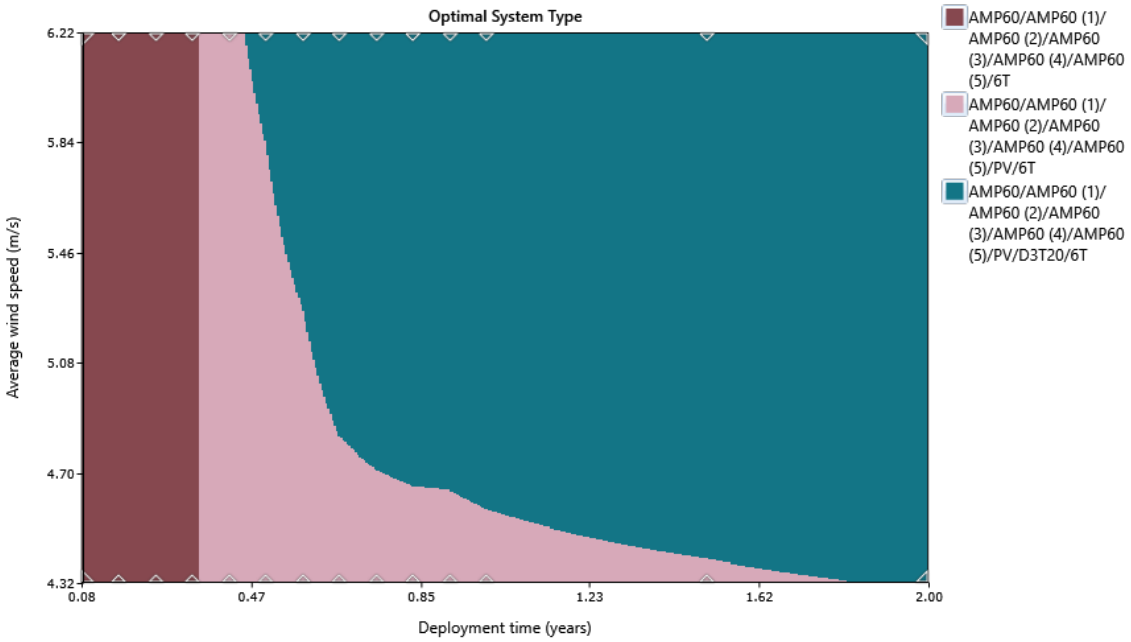

Figure 13. Transportation optimized microgrid architecture in high solar resource. Diesel generator only system is the maroon area, diesel plus PV in pink, and diesel, PV and wind in green.

To provide some more detail about the exact quantities of diesel generators, PV systems, and wind systems as a function of the transportation burden, the next plots show a different view of the same results. Figure 14 shows a collection of system architectures in a scenario of low solar and low wind resource. Figure 15 shows the same collection of system architectures but in a high solar and high wind resource. In each plot, the color of the line represents the number of wind turbines as indicated by the legend (dark red = 0 wind systems). Each dot along a single color represents an additional PV system from left to right. This shows all of the viable combinations of wind turbines and PV systems and their associated system transportation burden on the y-axis for different deployment lengths. In each case the point to the far left represents the baseline transportation burden that includes 0.78 truck trips for the diesel generators plus the fuel required to meet the load for the particular mission duration. Any system that falls below that point indicates that the addition of renewable generation is reducing the transportation burden as compared to diesel-only operation.

For the low solar and low wind scenarios presented in Figure 14, at 1 or 3 month durations, the addition of any PV and wind systems always leads to an increase in the overall transportation burden. At 6 months, for a given number of wind systems, adding up to 4 PV systems appears to decrease transportation burden and then increase its from there. The optimum architecture is zero wind and 3 or 4 PV systems. At 12 months, adding PV reduces the transportation burden for most cases with an optimum of zero wind and 7 PVs. This is all consistent with the analysis in Figure 12.

For the high solar and high wind scenarios presented in Figure 15, at 1 or 3 month durations, the PV and wind containers always increase overall transportation burden indicating they are not optimum to deploy for such short durations. At 6 months, for a given number of wind systems, adding about 4 PV systems leads to lower overall truck trips with 1-2 wind plus 3-4 PV systems

being optimum. At 12 months, adding additional wind and PV systems up to about 6-7 reduces the transportation burden, but sharply increases beyond that as more batteries are needed to capture periods of excess energy generation. This is all consistent with the analysis in Figure 13.

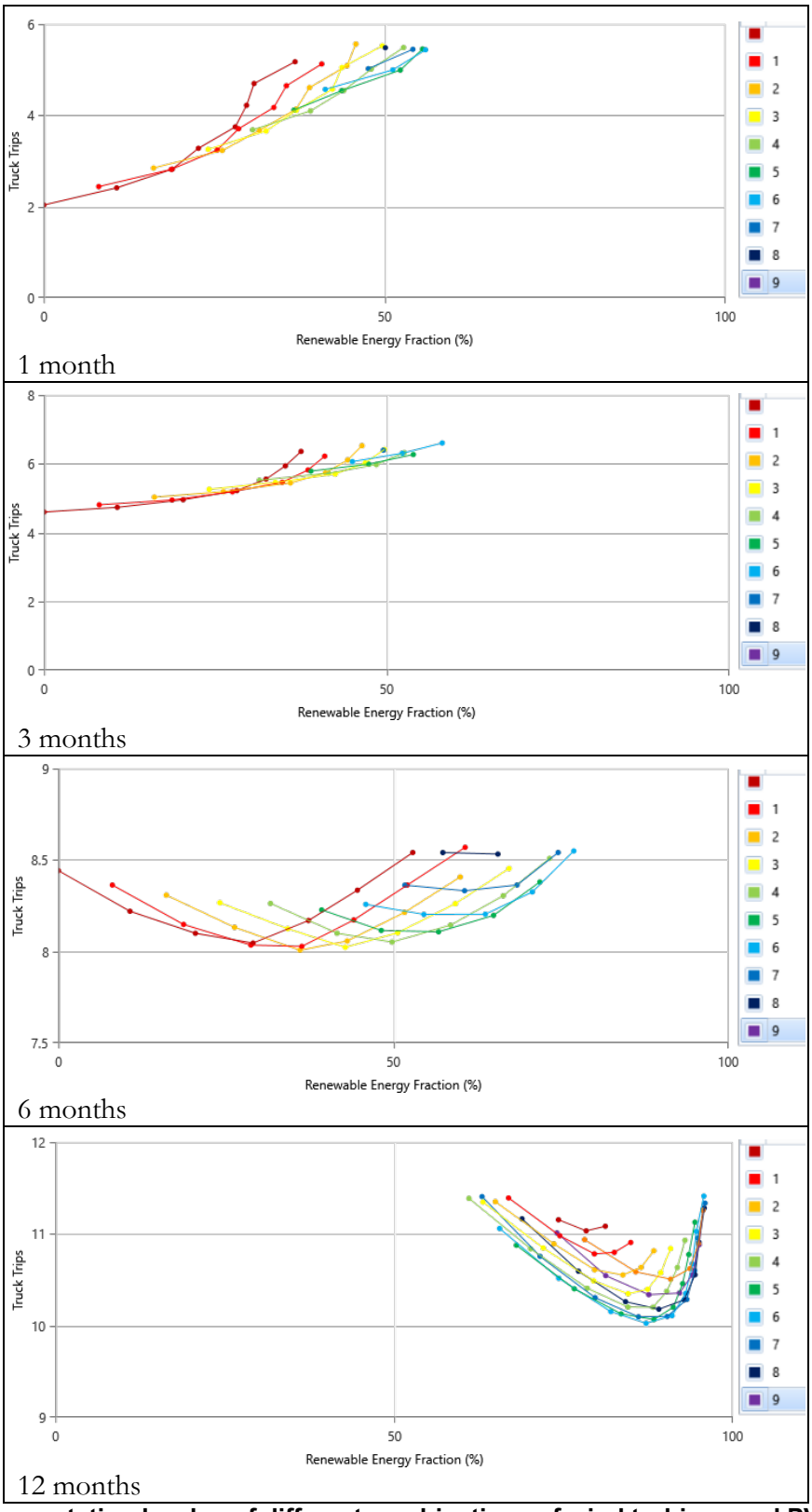

Figure 14. Transportation burden of different combinations of wind turbines and PV systems in a low solar and wind resource scenario for 1, 3, 6, and 12 months.

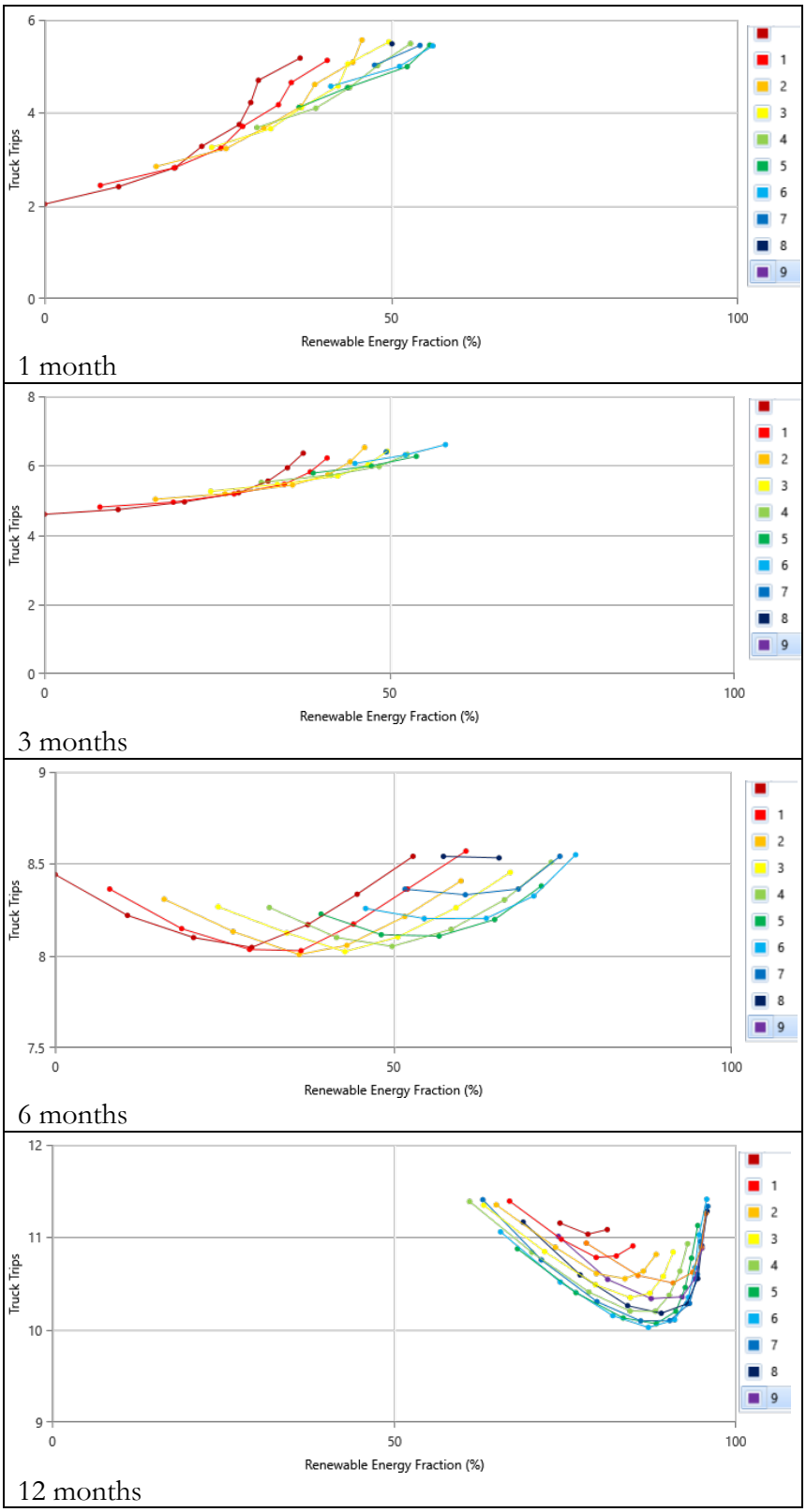

Figure 15. Transportation burden of different combinations of wind turbines and PV systems in a high solar and wind resource scenario for 1, 3, 6, and 12 months.

The final set of results highlight the optimization of battery storage for the different system architectures. In Figure 16, the optimum number of batteries for each combination of wind and PV system architectures is shown for 6 and 12 month deployments for both a low and high resource scenarios. In each plot, the color represents a fixed number of PV systems and the dots indicate the number of wind systems for that fixed amount of PV, increasing from left to right. The general observation is that increasing the number of PV systems (going generally from red through purple) results in the addition of more batteries than the addition of more wind systems (going left to right on a single color). In the 12-month deployment, high-resource scenario in the bottom figure, adding wind turbines can actually lead to a decrease in the number of batteries required for high numbers of PV systems (blue and purple colors). This is primarily a result of the fact that some wind is present statistically throughout the day, whereas the PV only produces when the sun is out, thus requiring more batteries to shift solar-generated power to meet evening and nighttime loads. A deeper look at what is called the complementarity of solar and wind resources is discussed in Section 3.2.

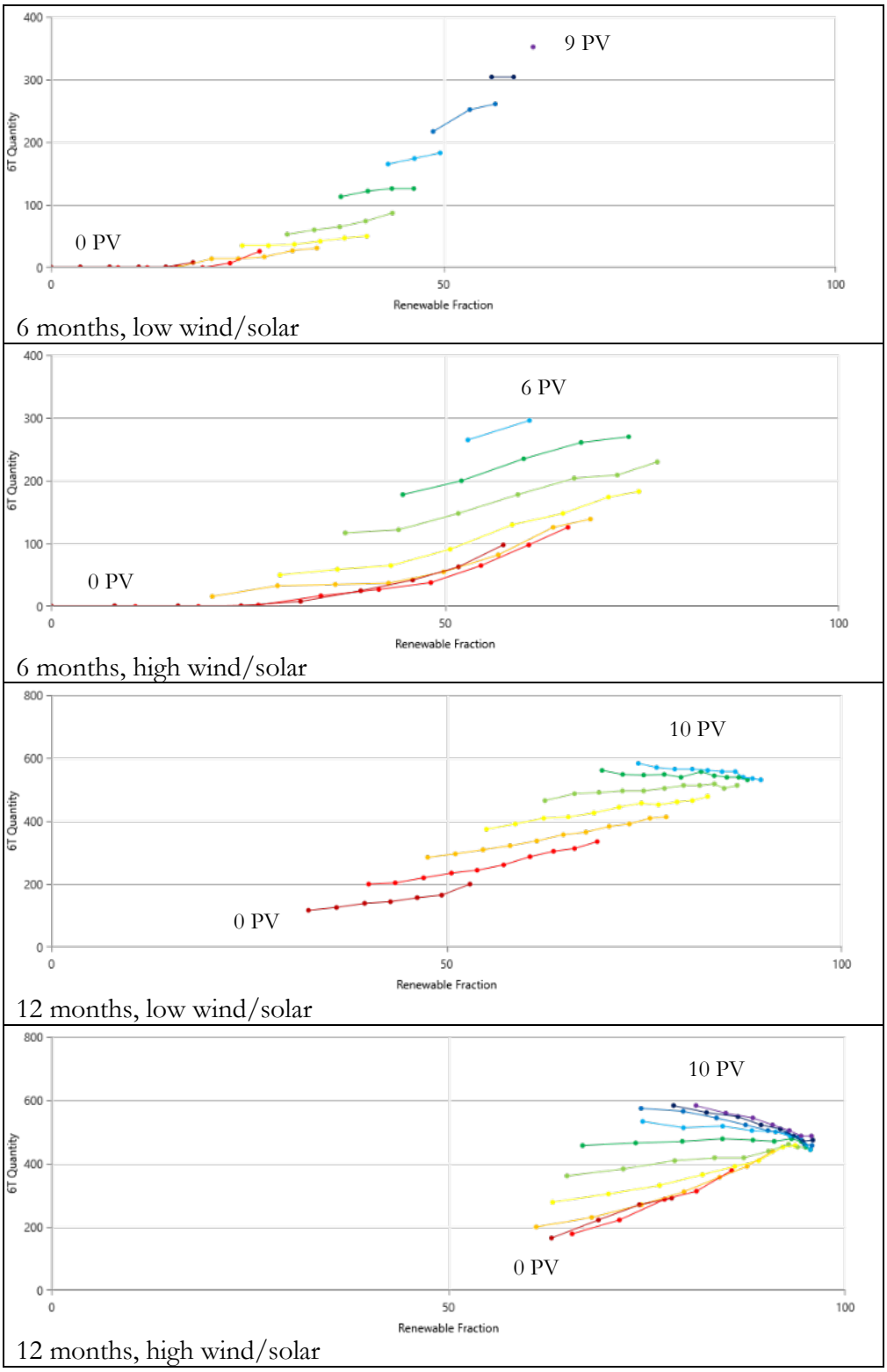

Figure 16. The quantity of 6T Li-Ion batteries deployed for each combination of wind and PV systems for 6- or 12-month durations at low wind and solar and high wind and solar resources. The color of the lines corresponds to the number of PV systems deployed with red indicating zero PV and purple a higher number as indicated with each dot along a single color representing an increasing number of wind turbine systems from left to right.

Figure 17 shows the impact of the number of 6T batteries on the total system transportation burden and excess (curtailed) renewable energy generation. Each line represents a combination of high or low wind and solar resource as indicated and the dots are different numbers of 6T batteries with the extremes shown in blue and the optimal number shown in green. The x-axes show the percent of excess electricity, which is a representation of how much wind and solar energy went unused because there was insufficient load to meet production and insufficient battery storage to store the excess. From a transportation perspective, too few batteries results in the need for more generation and therefore transportation burden and too many batteries results in more transportation burden to transport the extra batteries. The optimal number of batteries are within 30% of each other across the resource scenarios and the curve is relatively flat around each of the optimal battery sizes. This suggests a fixed number of batteries could be deployed regardless of the resource and be close to optimal.

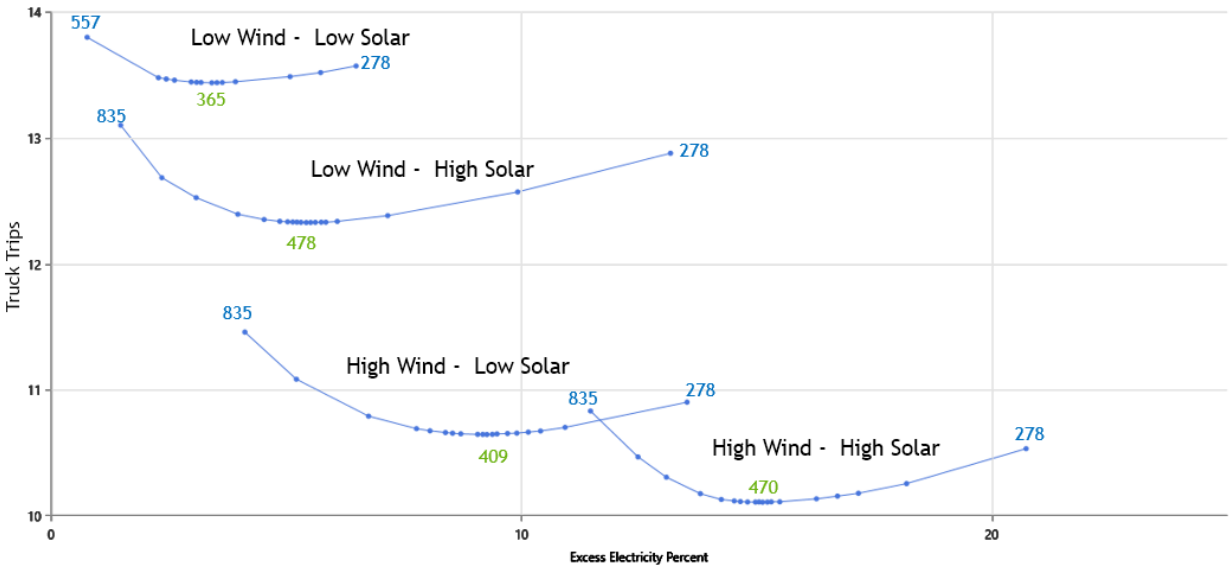

Figure 17. For each of the wind and solar resource combinations, the sensitivity of the number of batteries to the transportation burden is shown with the optimum number of 6T batteries in green text and the low and high extremes in blue.

3.1.3. Summary

The following general observations are noted for this section on transportation optimized microgrid architectures for the reference forward operating base model:

- PV containers have a shorter payback period than wind turbine containers in most scenarios and thus tend to be a component of transportation-optimized systems with shorter duration deployments (~4 months).
- Wind turbine containers can also become part of the transportation-optimized generation mix around 5 months in higher wind and lower solar resource locations.

- The optimal battery sizing is primarily driven by the amount of PV containers due to the larger energy production per container of PV versus Wind but also because the correlation of energy production and load of PV is lower than wind.
- The optimal battery sizing is a trade-off between having more storage to manage the mismatch between generation and load, versus less storage and more generation with more curtailment or excess energy production.

3.2. Seasonality and Complementarity Analysis Results

The second set of scenarios considered the impacts of mission duration and time of year or seasonality on the hybrid system performance. In the prior scenarios, the wind and solar resources were, on average, steady throughout the year. In this set of scenarios, the wind resource was still steady, but the solar resource was varied throughout the year by selecting a location in Croatia that is near 45 °N latitude, creating a significant difference in summer and winter performance. The other characteristic that was studied was the complementarity of the wind and solar resource. Resource complementarity is a concept of how two different resources, wind and solar in this case, provide a better match to the load when combined together as compared to either one separately [15]. Complementarity can happen on multiple time scales from daily to seasonally, and both will be examined in this section.

3.2.1. Diurnal Complementarity

The first set of results considered a full year of operation at the 45 °N latitude location with a range of wind speed resources ranging from low (4.32 m/s average) to high (6.22 m/s average). The search parameters were set to evaluate all combinations of wind, PV, and storage systems and optimize for the lowest overall transportation burden. Three sets of optimization simulations were run, with the wind resource having a daily peak at 12 pm, approximately concurrent with the solar resource, a wind peak at 6 pm, and at 12 am. These times were selected to explore the extreme bounds of wind and solar complementarity to represent the wide range of times when the wind speed peaks during the day depending on both location and time of year.

The results of the simulations are summarized in Table 13, grouped by the timing of the diurnal wind peak. As the wind speed peak shifts in time away from the noon solar peak, the optimum system architecture generally requires fewer truck trips, primarily due to the need for less battery storage because there is a better overall match between the generation and load. The optimal system architecture also tends towards more wind systems and fewer PV systems as the peaks of the two resources shift away from each other. Considering the highest wind resource (6.22 m/s) systems, the difference in transportation burden between a fully concurrent wind and solar peak (noon) and the maximally non-concurrent peak (midnight) is about 8% over a full year of operation. As the next section will demonstrate, this difference can be much more pronounced when looking at the impacts of seasonal variation in resource along with diurnal complementarity.

Table 13. Transportation optimized system architectures for different wind and solar resource complementarities.

Wind Speed Average (m/s)	PV kw (# containers)	Wind (# containers)	6T Battery (# containers)	Truck Trips	RE Fraction (%)	Total Fuel (L/yr)	PV (kWh/yr)	Wind (kWh/yr)
Noon wind resource peak (concurrent with solar resource peak)								
4.32	576 (9)	0	544 (5)	11.23	76	72,013	949,020	-
4.78	576 (9)	0	544 (5)	11.23	76	72,013	949,020	--
5.25	512 (8)	2	513 (5)	11.16	79	63,524	843,574	115,120
5.73	384 (6)	5	452 (4)	10.84	83	52,726	632,680	340,999
6.22	320 (5)	6	426 (4)	10.42	85	46,586	527,234	470,763
6pm wind resource peak								
4.32	576 (9)	0	544 (5)	11.23	76	72,013	949,020	-
4.78	576 (9)	0	544 (5)	11.23	76	72,013	949,020	-
5.25	448 (7)	3	487 (4)	11.12	79	64,673	738,127	172,814
5.73	384 (6)	5	444 (4)	10.68	84	50,187	632,680	341,263
6.22	320 (5)	6	413 (4)	10.16	86	42,762	527,234	470,897
12am wind resource peak								
4.32	576 (9)	0	544 (5)	11.23	76	72013	949,020	-
4.78	512 (8)	1	513 (5)	11.21	75	73881	843,574	46,814
5.25	384 (6)	5	378 (4)	10.83	81	58084	632,680	288,004
5.73	320 (5)	7	296 (3)	10.21	86	43024	527,234	477,677
6.22	256 (4)	7	239 (2)	9.60	86	45360	421,787	549,328

3.2.2. Seasonal Complementarity

The following results consider mission durations of 1 month, 3 months, and 12 months. For the 1-month and 3-month missions, the timing is set to occur during the lowest solar resource winter season and the highest solar resource summer season. As was plotted in Figure 11 previously, the lowest solar resource occurs in December with a daily radiation of 1.28 kWh/m^2/day and the highest occurs in July with a daily radiation of 7.36 kWh/m^2/day. This is a much larger variation than was considered in Section 3.1.2 where annual averages were used between 4.21 and 5.2 kWh/m^2/day. To facilitate direct comparisons of the resource variation, the system architecture was fixed for these scenarios with 6 wind systems, 6 PV systems, and 2 battery storage containers (500 total 6T batteries). From a transportation perspective, this fixed architecture results in 7 required truck trips.

For 1-month duration missions, depending on the time of year (low/high solar) and wind resource (low/high), the same system configuration (PV, wind, battery storage) reduced fuel consumption between 47% and 80% with total system truck trips between 9.68 and 8.26. For 3-month duration missions, the fuel reduction range is nearly the same, 47%-79% with total system truck trips between 11.03 and 8.81. For 1-year missions the fuel reduction range is from 65% to 73% with total system truck trips between 14.45 and 12.21. The first observation is that the shorter the mission duration, the more important it is to consider the seasonal resource variation and impact on performance. The

second observation is that the energy produced per PV container is generally higher than energy produced per wind system container except when the wind resource is high, and the solar resource is low in the winter months.

The above results are for a resource profile where the wind diurnal peak occurs at noon, concurrent with the PV peak. As in the prior section, these scenarios were repeated with the wind peak shifting to 6 pm and 12 am to assess the impacts. The general trends in fuel reduction are the same, however the fuel reduction in absolute percentage increases to a maximum of 88% in the 6pm case and 96% in the 12 am case as compared to the 80% reduction in the noon case. This result shows the importance of the complementarity of the wind and solar resource with increasing benefits as the wind and solar peak production shift away from each other, especially for shorter duration missions. The fuel and transportation burden results are summarized for a 1-month mission in Table 14 and the full results can be found in Appendix A.

Table 14. Summary of the seasonality and diurnal solar and wind resource complementarity variation on 1-month mission duration fuel and transportation burden

12 pm wind peak, 1-month mission			**6 pm wind peak, 1-month mission**			**12 am wind peak, 1-month mission**		
	Low Wind	High Wind		Low Wind	High Wind		Low Wind	High Wind
Low Solar	12,900 L Diesel 7.68 truck trips	9,222 L Diesel 7.49 truck trips	Low Solar	12,793 L Diesel 7.68 truck trips	8,155 L Diesel 7.43 truck trips	Low Solar	12,294 L Diesel 7.65 truck trips	6,748 L Diesel 7.36 truck trips
High Solar	5,265 L Diesel 7.28 truck trips	4,924 L Diesel 7.26 truck trips	High Solar	5,037 L Diesel 7.27 truck trips	2,842 L Diesel 7.15 truck trips	High Solar	3,241 L Diesel 7.17 truck trips	859 L Diesel 7.05 truck trips

3.2.3. Summary

The following general observations are noted for solar and wind resource complementarity:

- The impacts of the daily wind peak vs. solar peak primarily show up in terms of the optimal amount of battery storage. The further away in time the peaks in the two resources are, the better they match the load, requiring less storage and thus fewer truck trips.
- The time of year has a large impact on the system performance when considering missions shorter than 1 year. In the months with the lowest solar resource (November – January in the northern hemisphere) the energy output per wind turbine container exceeds that of PV containers in the high wind scenario. In all other scenarios, the energy output per PV container exceeds that of the wind container.

3.3. Mission Resilience Results

The mission resilience scenarios consider a situation where the supply of diesel fuel to the base is limited or interrupted to varying degrees. Like in Section 3.1, the location for this analysis is

equatorial, removing the seasonal variation in solar resource. The first set of results evaluates the impacts of limited fuel supply on the percent of unmet load given different resources and architectures. The second set of results considers a renewable system required to meet 100% of the critical loads of the base (priority 1 – 4 in Table 1). In the following results, the metric of "percent unmet load" is used as a proxy for mission resilience which was defined in Section 2.5.3. The percent unmet load is defined as the proportion of the total annual electrical load that went unserved because of insufficient generation.

3.3.1. Constrained Diesel Fuel and Unmet Loads

For these scenarios, the system architecture varies according to Table 15 but the total transportation burden is kept constant at 8 truck trips (16 20-foot ISO containers). In the base case described in 3.1.1, the total fuel consumption for 1 year with just diesel generators is 76,859 gallons. These set of simulations investigate diesel constraints that start at 20,000 gallons and drop to 0 gallons in 2500-gallon increments. Depending on the system architecture and the wind and solar resource, at some level there is insufficient diesel to power the generators to make up any deficits between the renewable generation and the load. To get a sense of how much load is unmet, there is a parameter in HOMER to allow capacity shortages. For these scenarios the allowable capacity shortage is set at 0, 1, 5, 10, 20, 30, 40, and 50%. Both low and high wind and solar resource were considered.

Table 15. Mission resilience system architectures

	Wind systems (containers)	PV systems (containers)	Battery containers (250 6T batteries per container)
Architecture 1	6	6	4
Architecture 2	12	0	4
Architecture 3	0	12	4

The results for each set of architectures are summarized in Figure 18, Figure 19, and Figure 20. The plots show that as the available diesel fuel approaches zero, the percent of unmet load increases for different architectures and renewable resource profiles. The best performing system is the hybrid system with 6 PV and 6 wind systems, except for the case of low wind and low solar where the 12 PV system slightly out-performs the 6Wind-6PV system. The general conclusion of this set of results is that systems that only include wind systems are unlikely to be as effective as those that also include some PV. More detailed results are provided in Appendix B.

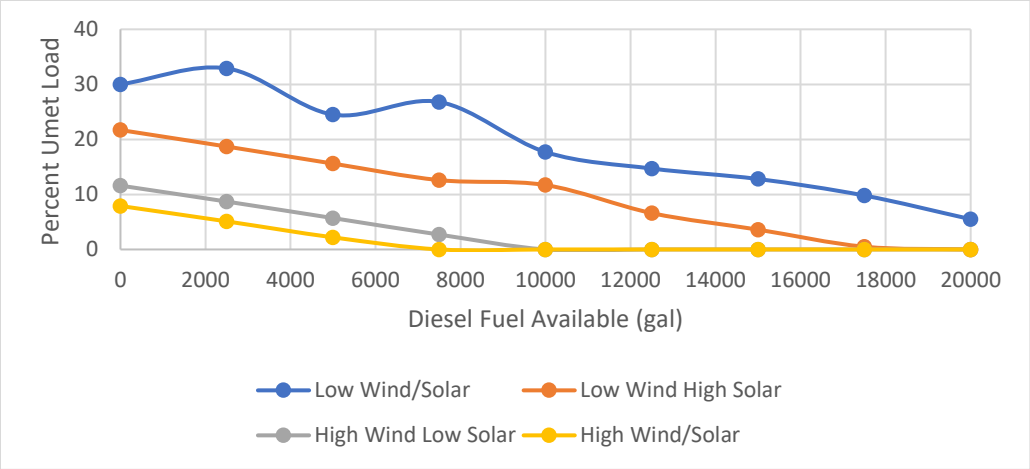

Figure 18. Percent unmet load for various levels of available diesel fuel and resource scenarios for a system architecture of 6 PV systems, 6 wind systems, and 4 battery containers.

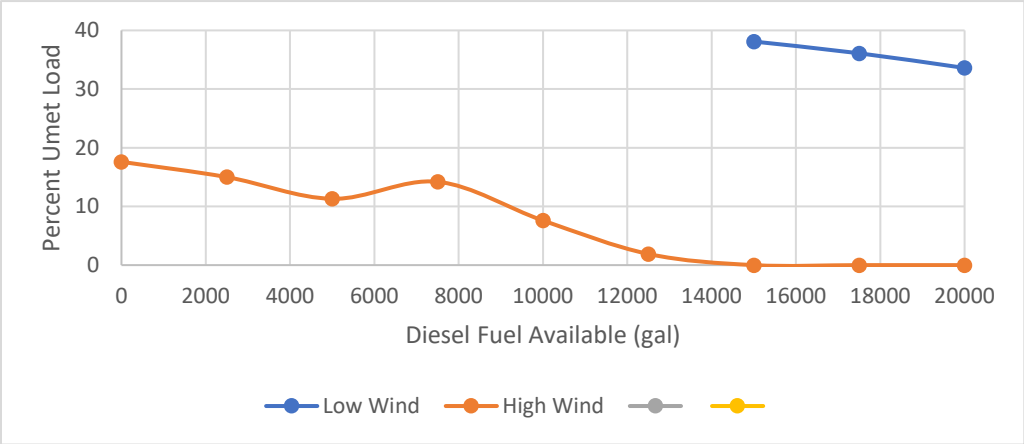

Figure 20. Percent unmet load for various levels of available diesel fuel and resource scenarios for a system architecture of 0 PV systems, 12 wind systems, and 4 battery containers.

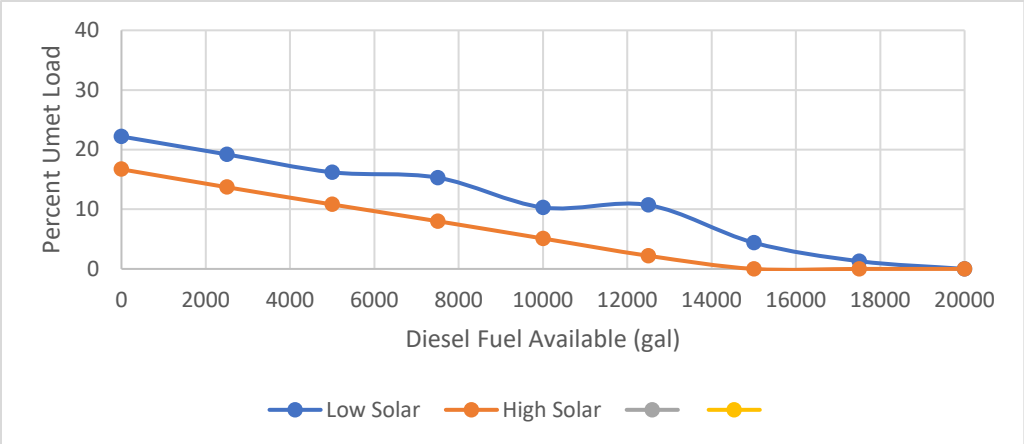

Figure 19. Percent unmet load for various levels of available diesel fuel and resource scenarios for a system architecture of 12 PV systems, 0 wind systems, and 4 battery containers.

3.3.2. *Mission Critical Loads*

In Section 2.1.2, the power system details of the reference base microgrid were presented including the order of mission critical loads. The top four critical loads at the base comprise about 22% of the overall base loads, so it is possible that a smaller renewable system that includes battery storage could maintain critical loads even without diesel fuel availability. For this analysis, the load profile for just the top four critical loads (Figure 21) was used to define an optimal system architecture that could provide 100% mission resilience. High and low solar resources were included but there was no diesel fuel availability.

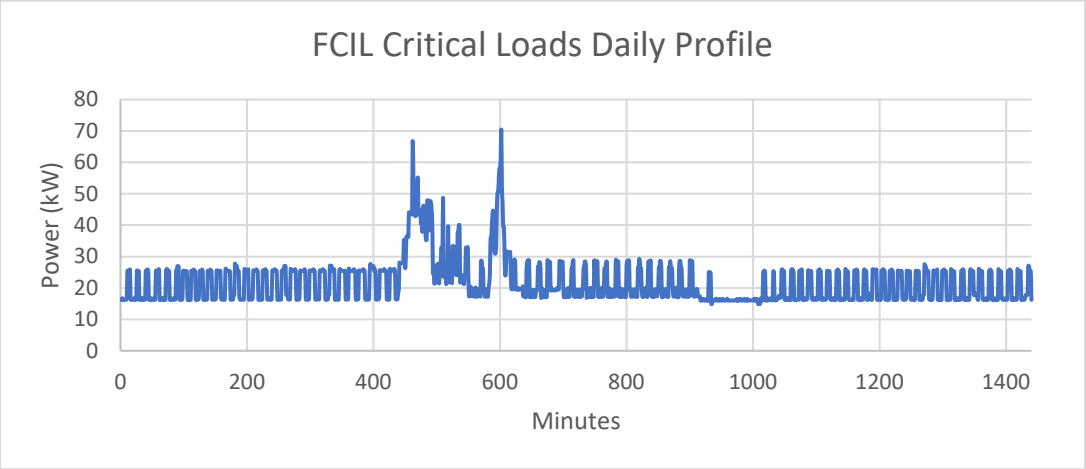

Figure 21. Daily load profile for the top four critical loads at the FCIL base model, representing about 22% of the overall base loads.

The results of the HOMER simulations are summarized in Table 16 which shows the optimal architecture that can meet 100% of the base critical loads without any diesel fuel consumption for the different wind and solar resource combinations. One interesting observation that stands out is that even in low wind scenarios, the optimal architecture still includes a wind system. This result did not occur in earlier scenarios that included the possibility of diesel generation. This provides another perspective on the potential benefit of hybrid wind and solar power systems for this application.

Table 16. Transportation-optimized systems that meet critical loads without diesel fuel.

Solar (kWh/m²/day)	Wind Speed (m/s)	PV systems	Wind turbine systems	Batteries	Truck Trips	PV Production (kWh/yr)	Wind Production (kWh/yr)	% of full base loads met by renewables
4.21	4.32	3	2	268	4.322	263,030	72,749	33
4.21	6.22	1	2	287	3.398	87,677	156,966	25
5.2	4.32	3	1	299	3.946	329,004	36,374	35
5.2	6.22	1	2	264	3.306	109,668	156,966	27

The same system architectures listed in Table 16 were also applied to a scenario where the full base load is present and also unlimited diesel fuel is available. The renewable systems meet between 25% and 35% of the overall base load as shown in the last column of Table 16. So, a system that is optimized to meet the critical loads (22% of overall load) 100% of the time can also provide an additional benefit of offsetting fuel when there is fuel available. Full simulation results are available in Appendix C with additional observations on the relative system configurations.

One final perspective on the resilience analysis with hybrid renewable systems is to consider the payback time for a fixed architecture of 3 PV systems and 2 wind systems and 268 6T batteries that is capable of meeting the critical loads in all of the resource scenarios considered, named here the "critical load renewable system". Table 17 shows the transportation burden (truck trips) for a diesel only system, and the critical load renewable system in low and high resource conditions. The mission duration steps up by 1 month increments to a full year. At month 7, the high resource scenario has a lower transportation burden than the diesel baseline and at month 9, the low resource scenario also reaches a lower transportation burden. From a resilience perspective, the critical load renewable system pays for itself on day one since there is no diesel fuel available to power the generators. From a transportation burden perspective, it would pay for itself no later than month 9.

Table 17. Transportation payback for the critical load renewable system in low and high resource.

Mission Duration (months)	Diesel only system (truck trips)	Critical load renewable system in low solar and wind resource (truck trips)	Critical load renewable system in high solar and wind resource (truck trips)
1	2.03	5.18	5.02
2	3.32	6.05	5.72
3	4.59	6.91	6.41
4	5.87	7.77	7.10
5	7.16	8.64	7.81
6	8.44	9.50	8.50
7	9.71	10.36	9.19
8	11.00	11.23	9.89
9	12.28	12.09	10.59
10	13.56	12.95	11.28
11	14.85	13.82	11.98
12	16.13	14.68	12.68

3.3.3. Summary

The following general observations are noted for this section on mission resilience:

- For a system with the same transportation burden having a system that is a mix of solar and wind energy generation performs better than either a pure solar or pure wind system at providing mission resilience (maximum uptime as a percentage of uptime plus downtime) when diesel fuel becomes limited.
- If a renewable system is designed to meet 100% of the critical load of a base, that system will offer maximum resilience to the critical loads and also be optimal for reducing overall fuel vs. just diesel systems, if missions last longer than 6-8 months, depending on the wind and solar resource.

3.4. Airborne Wind Results

For this final set of analyses, a model of a deployable airborne wind energy system was included along with the wind and PV system models used through the previous scenarios. The model was built using the assumptions provided in Section 2.2.2.2 where a 100 kW rated airborne wind system was assumed to fit into two 20-foot containers. The airborne system is designed to operate high off the ground at 200 meters and above. The wind speeds at this height are typically much greater than those closer to the ground, thus providing a big potential increase in power production. The same assumptions are used for the low and high wind resources in these scenarios; however, the average wind speed value is scaled up using a power law with an exponent of alpha = 0.14 which was found to match global data fairly well. The same 14% loss factor is assumed as the standard wind turbine and PV systems.

3.4.1. Simple Payback Analysis

A simple calculation was conducted on the airborne wind system to determine the rough payback time in terms of diesel fuel saved and transportation burden, similar to what was done in Section 3.1.1. For the calculation, the low wind speed of scenario of 4.32 m/s was scaled up to 200 m using the power law method which resulted in an average wind speed of 6.57 m/s. This results in an average power output of about 37 kW, thus requiring about 64 days to create the same 57,500 kWh of energy as a diesel generator using 5000 gallons of fuel. 5000 gallons is used for comparison here instead of 2500 gallons used in the prior payback analysis due to the fact that the airborne wind system requires two containers compared to the single container for the ground-based turbine. Scaling up the high wind speed to 200 m results in an average wind speed of 9.47 m/s which would produce 74 kW of power by the airborne wind system. The payback time drops to only 32 days for this scenario. These are both significantly shorter times than was calculated for the standard PV and wind turbine systems.

3.4.2. HOMER Transportation-Optimized Systems

Similar to Section 3.1.2, HOMER was used to identify the system architectures that minimize transportation burden for high and low wind and solar resources, but now with the option to select the airborne wind system in addition to the prior components. The results of the low solar resource scenario (Figure 22, top) show that at around 2 months, airborne wind systems begin to be selected as part of the optimal architecture and PV systems are not selected until after 7 months in the lowest

wind resource. In the high solar scenario (Figure 22, bottom) the trend for airborne wind is similar, however PV becomes viable about a month sooner at 6 months and at slightly higher wind resources. The standard 25 kW ground-mounted turbine is not selected as part of an optimized system in any scenario. Table 18 shows a direct calculation of the annual energy production of the PV system, the standard wind system, and the airborne wind system, all scaled to the same transportation size of two 20-foot containers. The modeled performance of the airborne wind system is impressive compared to the standard wind system and the PV system, however it's important to note that this is also the least mature technology and very little independent performance verification testing has occurred on any airborne wind system. These results should be taken with a sufficient amount of uncertainty about the real-world performance, especially in a deployable application. However, it does stand out as an interesting technology to consider especially for a rapidly deployable application where the available wind resources on site are not well known and typically low closer to the ground.

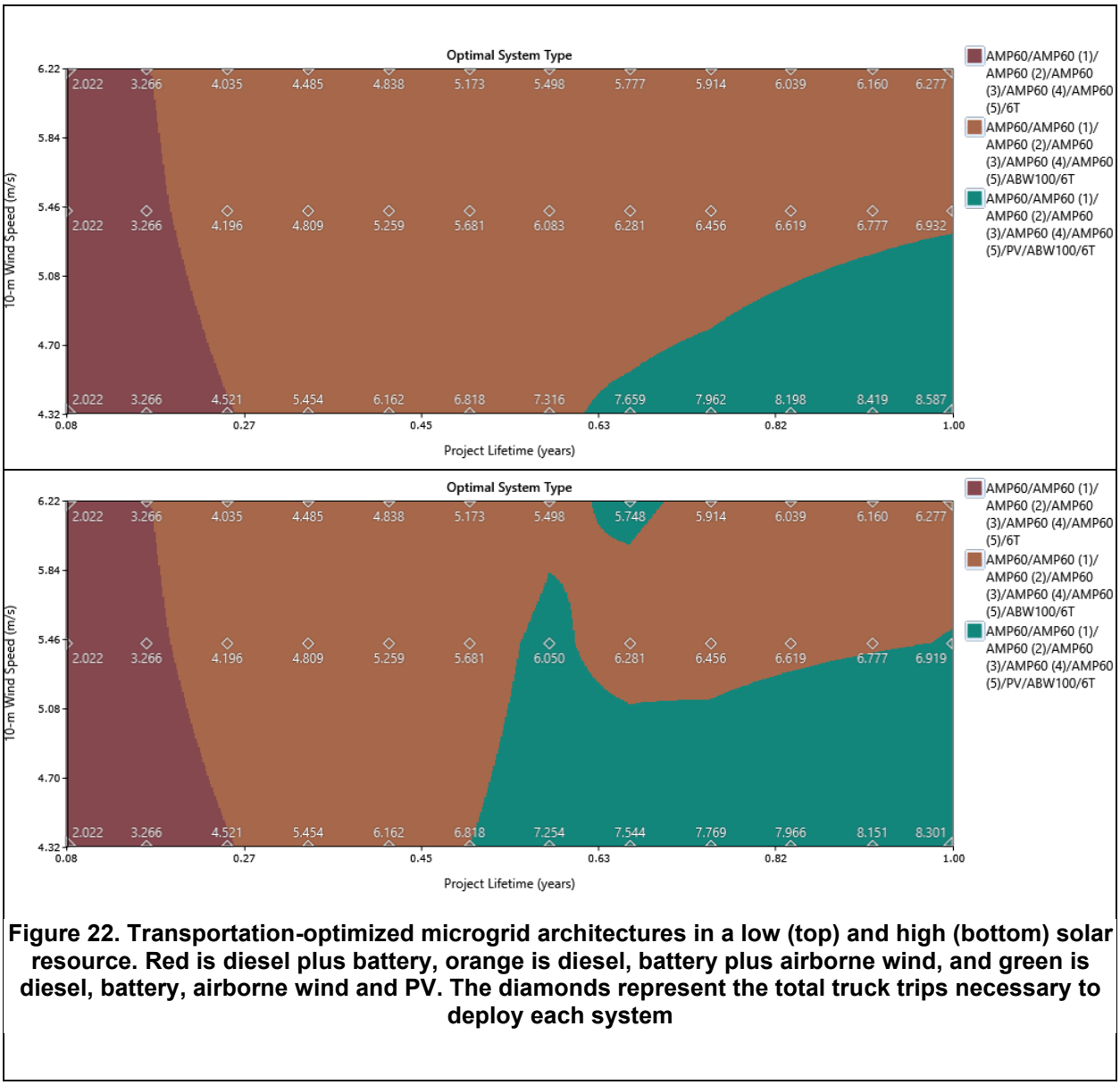

Figure 22. Transportation-optimized microgrid architectures in a low (top) and high (bottom) solar resource. Red is diesel plus battery, orange is diesel, battery plus airborne wind, and green is diesel, battery, airborne wind and PV. The diamonds represent the total truck trips necessary to deploy each system

Table 18. Comparative 1-year performance of the different renewable generator models.

Resource Profile	2 PV system containers annual production (kWh)	2 Standard wind system containers annual production (kWh)	1 Airborne wind energy system in 2 Containers annual production (kWh)
Low wind /solar resource	175,353	72,644	272,026
Low wind / high solar resource	219,336	72,644	272,026
High wind / high solar resource	219,336	156,831	412,132

3.4.3. Summary

The following general observations are noted for this section on airborne wind:

- Transportation-optimized system architectures include airborne wind systems as soon as 2-3 months and generally do not incorporate PV in addition to that until 6-8 months. This is a much quicker payback for airborne wind systems than either the standard wind system or PV system.
- The airborne wind system (2 containers) produces more power than two of the ground-based wind turbine containers. In low wind resources, the airborne system produces approximately 3.7 times more energy than the ground-based turbine and in high wind, produces 2.6 times more energy.
- The results for the airborne wind model are impressive, but the technology is the most immature of the three technologies considered and extensive independent field-testing verification should be conducted to build confidence in the potential of airborne wind for deployable applications.

This page left blank

4. CONCLUSIONS

The general objective of this study was to quantify the potential value of a deployable wind system in terms of mission-relevant metrics like transportation burden and mission resilience under a wide range of both environmental conditions found across the world and integrated with a variety of other distributed energy resources including diesel generators, photovoltaics, and battery storage. The approach explored bounding cases of high and low resources for wind and solar that occur on the vast majority of the Earth's landmass and system architectures that varied from all diesel generation to all renewable generation. This broad search space is intended to highlight general characteristics and to find where a deployable wind system can provide clear value. It was not intended to design an optimal system for a specific base with a specific mission.

One of the biggest challenges when considering alternatives to fossil fuels for Department of Defense operational energy needs is working within the existing systems, both physical infrastructure and planning and operations. Like our domestic energy systems, military systems have been designed around the high energy density, complex, and more centralized supply chain of fossil fuels. Renewable energy systems like wind and solar require very different hardware, and different planning and operational strategies to maximize their potential. Simply dropping in wind or solar energy system into the existing diesel-powered systems is unlikely to provide much apparent value.

Mission resilience may provide a better perspective and approach to evaluate the role of renewable energy. Diesel fuel is difficult to surpass in terms of a mobile and deployable energy source. It transports and stores compactly and provides reliable power on site in a wide range of conditions. But diesel is also entirely dependent on a complex supply chain that can be disrupted in a variety of ways. When the fuel runs out, there is no power at all. A well-designed deployable system incorporating wind, solar, and battery storage can provide continuous, on-site energy for a mission-critical load and still meet mobility and ease of use requirements.

As a result of the modeling and simulation scenarios explored in this study, the following general conclusions provide some guidance as to where deployable wind systems can provide unique value.

The average wind resource varies widely across the world and even within a single location through the day or year. The available power in the wind scales with the cube of the wind speed, so a doubling of wind speed increases the available power by 8-fold. This very nonlinear characteristic of wind energy means that wind systems perform significantly better in higher wind resource than in low resources. Photovoltaic systems don't have as wide a range in performance except in higher latitudes where seasonally they can vary significantly, for instance summer to winter.

Hybrid wind-PV systems generally outperform either just wind or just PV systems. Wind energy can be a very valuable complement to a PV system depending on the load profile and resource characteristics especially for mission durations of 5 months or more. If there is a significant load at night, the addition of wind energy to a PV-only system produces power at night especially where a strong evening or nighttime diurnal wind speed peak occurs and reduces the need for battery storage. A location with a diurnal wind peak at midnight versus a peak at noon will favor a system with more wind, less PV, and less batteries, reducing overall transportation burden by 8% in a high wind scenario. Seasonally, a wind turbine may also provide significant value, most notably in higher latitudes in the winter months. In the months with the lowest solar resource (November – January in the northern hemisphere) the energy output per wind turbine container exceeds the energy per PV container by 35% in the high wind scenario.

When considering mission resilience, wind systems are a highly valuable complement to PV systems. When diesel fuel is readily accessible, it takes a longer time for a wind system to pay for itself in terms of a transportation burden, especially in a lower wind resource location. However, when diesel becomes unreliable or unavailable, even in a low wind location, optimal architectures designed to meet 100% of the critical load include roughly equal numbers of wind and PV systems. These same systems when operated alongside diesel generators during normal base operations can offset as much as 35% of the diesel fuel consumption.

Airborne wind energy systems show strong potential to be a particularly good fit for defense and disaster deployment applications. The ability of airborne wind energy systems to access stronger and more consistent winds in much higher altitudes than tower-mounted wind turbines is a major benefit. The airborne system energy generation per unit of transportation is higher than wind, PV, and even diesel generation on all but the shortest duration missions (< 2 months). The airborne wind system (2 containers) produces more power than two of the ground-based wind turbine containers. In low wind resources, the airborne system produces approximately 3.7 times more energy than the ground-based turbine and in high wind, produces 2.6 times more energy.

These conclusions support the potential value of deployable wind to mission needs. The next step is to create opportunities to demonstrate deployable wind technologies in a relevant field environment to help validate performance and identify specific areas where additional improvements are needed. Testing locations that have an existing microgrid capable of integrating deployable wind and solar power (e.g. FCIL) would be particularly useful to understand the benefits and technical challenges of deployable hybrid power systems.

REFERENCES

[1] B. Naughton, T. Brown, S. Gilletly and C. Kelley, "Computational analysis of depoyable wind turbine systems in defense operational energy applications," Sandia National Laboratories, Albuquerque, 2020.

[2] The Under Secretary of Defense, "Memorandum on Metrics and Standards for Energy Resilience at Military Installations," Department of Defense, Washington, D.C., 2020.

[3] U.S. Army, "ATP 4-45 (FM 4-20.07) Force Provider Operations," 2014.

[4] U.S. Army, "Advanced Medium Mobile Power Source (AMMPS) Microgrid," 02 11 2021. [Online]. Available: https://asc.army.mil/web/portfolio-item/cs-css-advanced-medium-mobile-power-source-ammps-microgrid/.

[5] US Marine Corps, "GENERATOR SET, 60 KW, 60 HZ, AMMPS, SKID MOUNTED," 16 09 2021. [Online]. Available: https://www.marcorsyscom.marines.mil/Portals/105/PfM/LCES/ES/Power%20Team/Mobile%20Power/Info%20Sheets/GENERATORSET60KW60HZAMMPSSKIDMOUNTED.pdf.

[6] B. Naughton, T. Jimenez, R. Preus, B. Summerville, B. Whipple, D. Reen, J. Gentle and E. Lang, "Design Guidelines for Deployable Wind Turbines for Military Operational Energy Applications," Sandia National Laboratories SAND2021-14581 R, 2021.

[7] World Bank, "Global Wind Atlas," [Online]. Available: https://globalwindatlas.info/. [Accessed 06 12 2019].

[8] Epsilor, "ELI-52526-B NATO Li-Ion Rechargeable Battery Specifications," 16 09 2021. [Online]. Available: https://www.epsilor.com/wp-content/uploads/2020/04/ELI-52526-B_6T_Battery_Datasheet_Rev_2.pdf.

[9] HOMER, "HOMER Pro v3.13 User Manual - Synthetic Wind Data," [Online]. Available: https://www.homerenergy.com/products/pro/docs/3.13/generating_synthetic_wind_data.html. [Accessed 15 06 2020].

[10] G. Ren, J. Wan and W. Wang, "Quantitative insights into the differences of variability and intermittency between wind and solar resources on spatial and temporal scales in China," *J. Renewable Sustainable Energy,* vol. 13, 2021.

[11] M. Cui, J. Zhang, C. Feng, A. R. Florita, Y. Sun and B.-M. Hodge, "Characterizing and analyzing ramping events in wind power, solar power, load, and netload," *Renewable Energy,* vol. 111, pp. 227 - 244, 2017.

[12] C. A. Cañizares, "Trends in Microgrid Control," *IEEE Transactions on Smart Grid,* vol. 5, pp. 1905 - 1919, 2014.

[13] HOMER, "HOMER Pro v3.13 User Manual - Wind Data Histograms," [Online]. Available: https://www.homerenergy.com/products/pro/docs/3.13/wind_data_histograms.html. [Accessed 15 06 2020].

[14] Solargis s.r.o. on behalf of the World Bank Group, "Global Solar Atlas 2.0," 18 09 2021. [Online]. Available: https://globalsolaratlas.info/.

[15] Y. Li, V. G. Agelidis and Y. Shrivastava, "Wind-Solar Resource Complementarity and its Combined Correlation with Electricity Load Demand," *The 4th IEEE Conference on Industrial Electronics and Applications,* pp. 3623 - 3628, 2009.

[16] Small Wind Certification Council, "ICC-SWCC Summary Report LPP-16-05 (Bergey Excel 15)," 2019.

[17] Bergey Windpower Co., "Owner's Manual for BWC Excel 15 Wind Turbine & Powersync III Inverter Rev. 0," 2018.

[18] C. L. Archer and M. Z. Jacobson, "Evaluation of Global Wind Power," *Journal of Geophysical Research,* vol. 110, p. D12110, 2005.

[19] Department of the Army, "Army Container Operations FM 55-80," 1997.

[20] U. Army, "Heavy Expanded Mobility Tactical Truck Program," [Online]. Available: https://asc.army.mil/web/portfolio-item/cs-css-heavy-expanded-mobility-tactical-truck-hemtthemtt-extended-service-program-esp/.

[21] P. Jamieson, Innovation in Wind Turbine Design, John Wiley & Sons, Ltd, 2011.

[22] U. A. Headquarters, "BASE CAMPS ATP 3-37.10," 2017.

[23] Energy Information Administration, "Electricity generation, capacity, and sales in the United States," [Online]. Available: https://www.eia.gov/energyexplained/electricity/electricity-in-the-us-generation-capacity-and-sales.php. [Accessed 29 06 2020].

[24] U.S. Department of Defense, "2018 National Defense Strategy of The United States of America," 2019.

APPENDIX A. FULL RESULTS FROM SEASONALITY ANALYSIS

Table 19. Seasonality analysis for 1-month and 3-month missions with wind and solar resource peak both occurring at 12 pm

	Wind peak at noon									
	1-month deployment				3-month deployment				1-year deployment	
	Lowest Solar Resource		Highest Solar Resource		Lowest Solar Resource		Highest Solar Resource			
Parameter	Average Hourly Value (4.32 wind, December)	Average Hourly Value (6.22 wind, December)	Average Hourly Value (4.32 wind, July)	Average Hourly Value (6.22 wind, July)	Average Hourly Value (4.32 wind, Nov-Jan)	Average Hourly Value (6.22 wind, Nov-Jan)	Average Hourly Value (4.32 wind, Jun-Aug)	Average Hourly Value (6.22 wind, Jun-Aug)	Average Hourly Value (4.32 wind)	Average Hourly Value (6.22 wind)
Avg Load Served (kW)	111.3	111.3	111.3	111.3	111.3	111.3	111.3	111.3	111.3	111.3
Avg PV generation (kW)	39.7	39.7	101.5	101.5	40.9	40.9	97.3	97.3	72.2	72.2
Avg Generation Per PV container (kW)	6.6	6.6	16.9	16.9	6.8	6.8	16.2	16.2	12.0	12.0
Avg wind generation (kW)	24.9	53.8	24.9	53.8	24.9	53.8	24.9	53.8	24.8	53.7
Avg Generation Per wind container (kW)	4.1	9.0	4.1	9.0	4.1	9.0	4.1	9.0	4.1	9.0
Avg Battery Charge (kW)	18.6	29.4	34.4	30.9	17.8	28.7	33.1	31.0	26.8	30.2
Avg Battery Discharge (kW)	16.7	26.5	30.9	27.7	16.0	25.8	29.8	27.8	24.2	27.2
Avg Diesel Generator (kW)	56.3	43.3	22.3	23.1	56.6	43.4	24.6	24.1	37.9	31.7
Diesel Fuel (L/hr)	17.3	12.4	7.1	6.6	17.4	12.4	7.8	6.9	11.8	9.1
Total Fuel (L)	12900	9222	5265	4924	38462	27416	17120	15296	103197	79738
Fuel Truck Trips (=5000 gal)	0.68	0.49	0.28	0.26	2.03	1.45	0.90	0.81	5.45	4.21
Equipment Truck Trips (6)	7.00	7.00	7.00	7.00	7.00	7.00	7.00	7.00	7.00	7.00
Total Truck Trips	7.68	7.49	7.28	7.26	9.03	8.45	7.90	7.81	12.45	11.21
Baseline Fuel Use (L)	24245	24245	24245	24245	72735	72735	72735	72735	290943	290943
Baseline Truck Trips	1.28	1.28	1.28	1.28	3.84	3.84	3.84	3.84	15.37	15.37
Fuel Reduction (%)	47%	62%	78%	80%	47%	62%	76%	79%	65%	73%

Table 20. Seasonality analysis for 1-month and 3-month missions with wind and solar resource peaks at 6 pm and 12 pm respectively

	Wind peak at 6pm									
	1-month deployment				3-month deployment				1-year deployment	
	Lowest Solar Resource		Highest Solar Resource		Lowest Solar Resource		Highest Solar Resource			
Parameter	Average Hourly Value (4.32 wind, December)	Average Hourly Value (6.22 wind, December)	Average Hourly Value (4.32 wind, July)	Average Hourly Value (6.22 wind, July)	Average Hourly Value (4.32 wind, Nov-Jan)	Average Hourly Value (6.22 wind, Nov-Jan)	Average Hourly Value (4.32 wind, Jun-Aug)	Average Hourly Value (6.22 wind, Jun-Aug)	Average Hourly Value (4.32 wind)	Average Hourly Value (6.22 wind)
Avg Load Served (kW)	111.3	111.3	111.3	111.3	111.3	111.3	111.3	111.3	111.3	111.3
Avg PV generation (kW)	39.7	39.7	101.5	101.5	40.9	40.9	97.3	97.3	97.3	72.2
Avg Generation Per PV container (kW)	6.6	6.6	16.9	16.9	6.8	6.8	16.2	16.2	16.2	12.0
Avg wind generation (kW)	24.7	53.6	24.7	53.6	24.7	53.6	24.7	53.6	24.7	53.8
Avg Generation Per wind container (kW)	4.1	8.9	4.1	8.9	4.1	8.9	4.1	8.9	4.1	9.0
Avg Battery Charge (kW)	18.9	21.6	34.5	30.0	17.8	21.6	33.5	29.7	33.5	26.9
Avg Battery Discharge (kW)	17.0	19.4	30.8	26.5	16.1	19.4	30.1	26.4	30.1	24.3
Avg Diesel Generator (kW)	56.1	35.0	21.3	11.9	56.5	34.1	23.2	12.8	23.2	20.6
Diesel Fuel (L/hr)	17.2	11.0	6.8	3.8	17.4	10.7	7.3	4.1	7.3	6.5
Total Fuel (L)	12793	8155	5037	2842	38348	23527	16158	9053	64104	57087
Fuel Truck Trips (=5000 gal)	0.68	0.43	0.27	0.15	2.03	1.24	0.85	0.48	3.39	3.02
Equipment Truck Trips (6)	7.00	7.00	7.00	7.00	7.00	7.00	7.00	7.00	7.00	7.00
Total Truck Trips	7.68	7.43	7.27	7.15	9.03	8.24	7.85	7.48	10.39	10.02
Baseline Fuel Use (L)	24245	24245	24245	24245	72735	72735	72735	72735	290943	290943
Baseline Truck Trips	1.28	1.28	1.28	1.28	3.84	3.84	3.84	3.84	15.37	15.37
Fuel Reduction (%)	47%	66%	79%	88%	47%	68%	78%	88%	78%	80%

Table 21. Seasonality analysis for 1-month and 3-month missions with wind and solar resource peaks at 12 am and 12 pm respectively

	Wind peak at midnight									
	1-month deployment				3-month deployment				1-year deployment	
	Lowest Solar Resource		Highest Solar Resource		Lowest Solar Resource		Highest Solar Resource			
Parameter	Average Hourly Value (4.32 wind, December)	Average Hourly Value (6.22 wind, December)	Average Hourly Value (4.32 wind, July)	Average Hourly Value (6.22 wind, July)	Average Hourly Value (4.32 wind, Nov-Jan)	Average Hourly Value (6.22 wind, Nov-Jan)	Average Hourly Value (4.32 wind, Jun-Aug)	Average Hourly Value (6.22 wind, Jun-Aug)	Average Hourly Value (4.32 wind)	Average Hourly Value (6.22 wind)
Avg Load Served (kW)	111.3	111.3	111.3	111.3	111.3	111.3	111.3	111.3	111.3	111.3
Avg PV generation (kW)	39.7	39.7	101.5	101.5	40.9	40.9	97.3	97.3	72.2	72.2
Avg Generation Per PV container (kW)	6.6	6.6	16.9	16.9	6.8	6.8	16.2	16.2	12.0	12.0
Avg wind generation (kW)	24.8	53.7	24.8	53.7	25.1	53.9	24.9	53.7	24.9	53.8
Avg Generation Per wind container (kW)	4.1	8.9	4.1	9.0	4.2	9.0	4.1	9.0	4.1	9.0
Avg Battery Charge (kW)	16.9	19.3	32.6	21.5	15.6	18.4	30.5	22.0	24.4	21.2
Avg Battery Discharge (kW)	15.2	17.2	29.3	19.1	14.4	16.9	27.5	19.9	22.1	19.1
Avg Diesel Generator (kW)	53.3	28.8	13.3	3.4	52.9	27.6	17.1	4.7	32.0	14.1
Diesel Fuel (L/hr)	16.5	9.1	4.4	1.2	16.4	8.7	5.5	1.6	10.1	4.6
Total Fuel (L)	12294	6748	3241	859	36252	19285	12133	3430	88255	39904
Fuel Truck Trips (=5000 gal)	0.65	0.36	0.17	0.05	1.92	1.02	0.64	0.18	4.66	2.11
Equipment Truck Trips (6)	7.00	7.00	7.00	7.00	7.00	7.00	7.00	7.00	7.00	7.00
Total Truck Trips	7.65	7.36	7.17	7.05	8.92	8.02	7.64	7.18	11.66	9.11
Baseline Fuel Use (L)	24245	24245	24245	24245	72735	72735	72735	72735	290943	290943
Baseline Truck Trips	1.28	1.28	1.28	1.28	3.84	3.84	3.84	3.84	15.37	15.37
Fuel Reduction (%)	49%	72%	87%	96%	50%	73%	83%	95%	70%	86%

APPENDIX B. RESILIENCE SCENARIO RESULTS

Each architecture set was simulated with the two resource scenarios for the range of diesel availability and allowable capacity shortage. The results are shown graphically in Figure 23, Figure 24, and Figure 25.

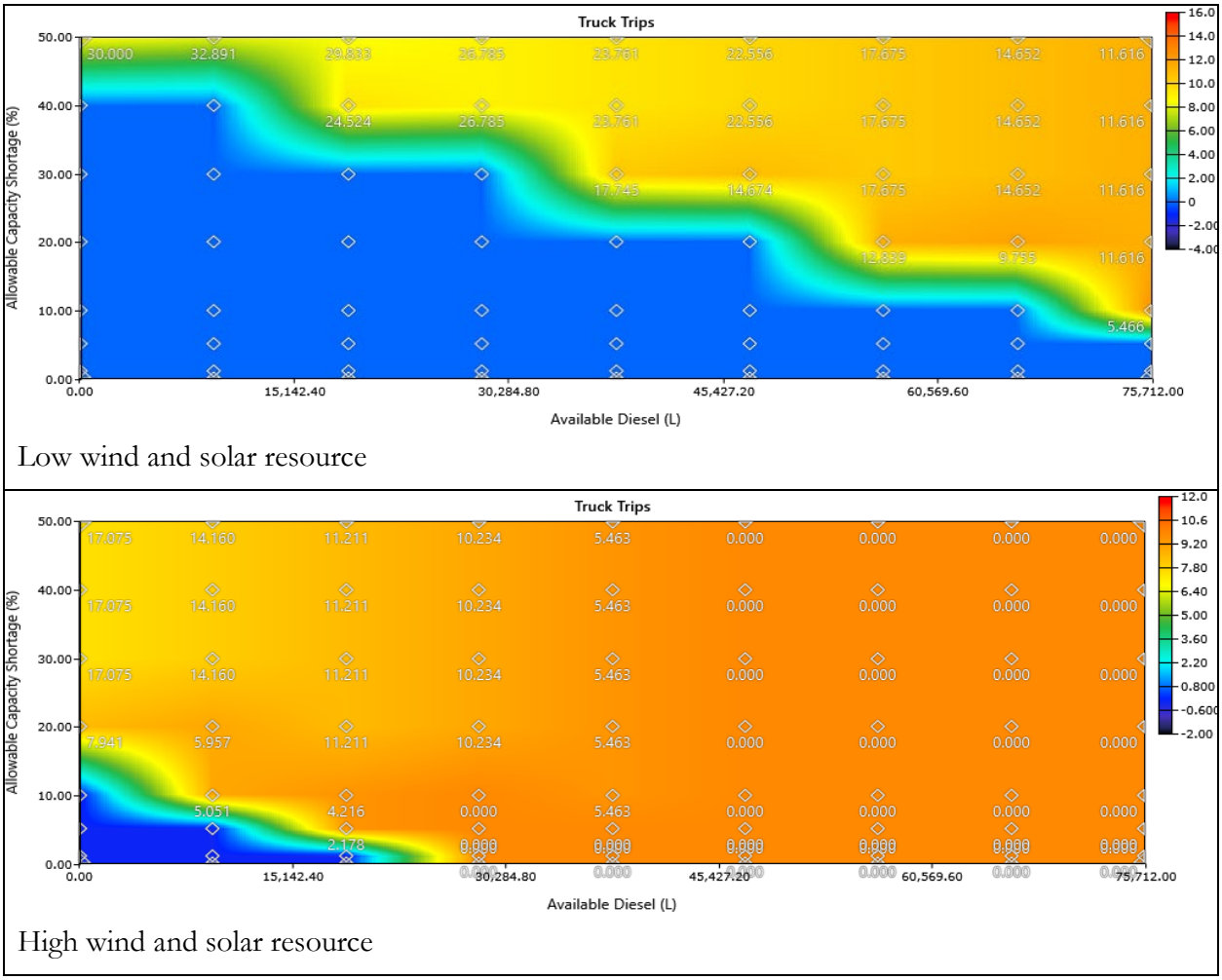

Figure 23. Percent unmet load (diamonds) for various levels of diesel fuel availability for a system architecture consisting of 6 wind systems, 6 PV systems, and 4 battery storage containers

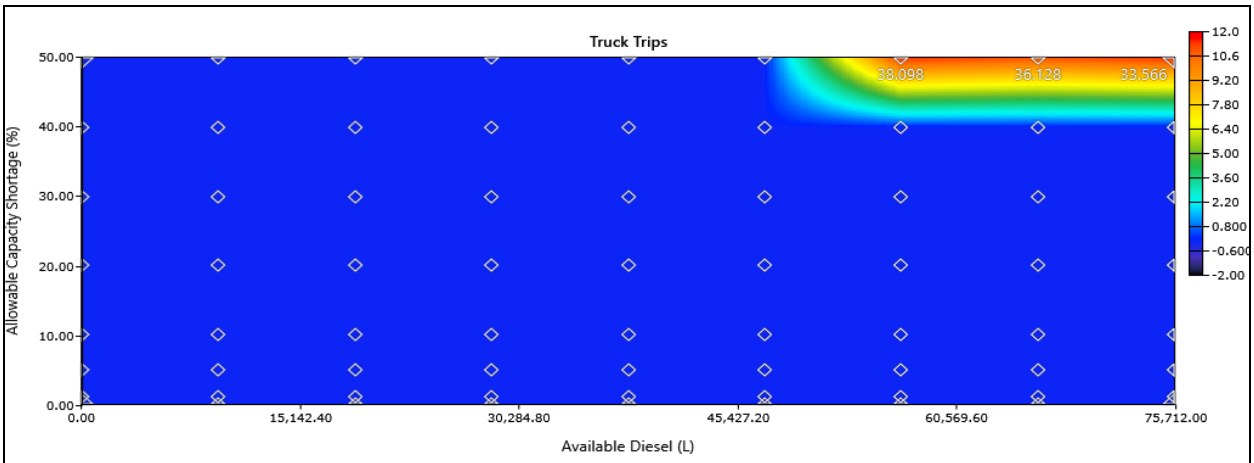

Low wind and solar resource

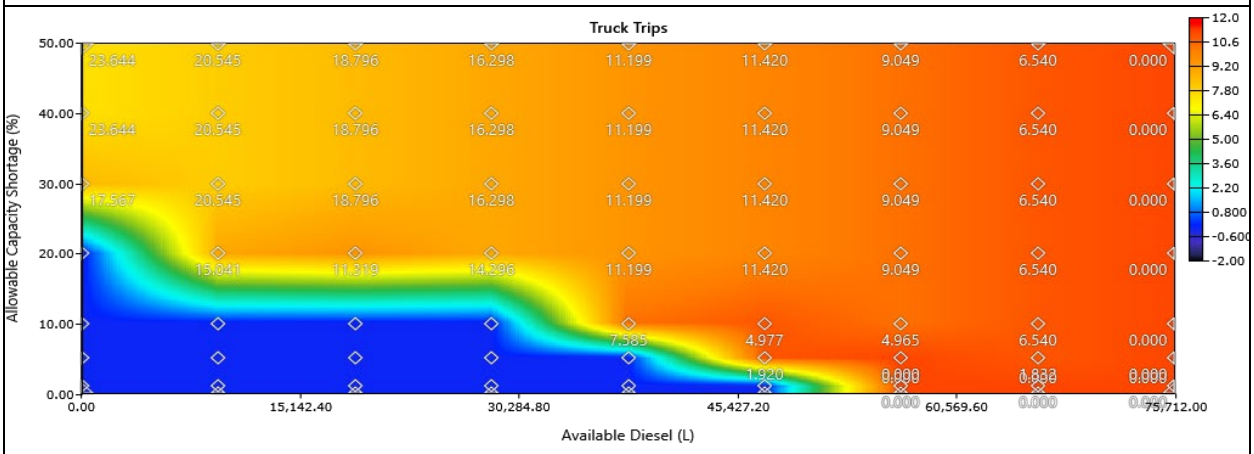

High wind and solar resource

Figure 24. Percent unmet load (diamonds) for various levels of diesel fuel availability for a system architecture consisting of 12 wind systems, 0 PV systems, and 4 battery storage containers

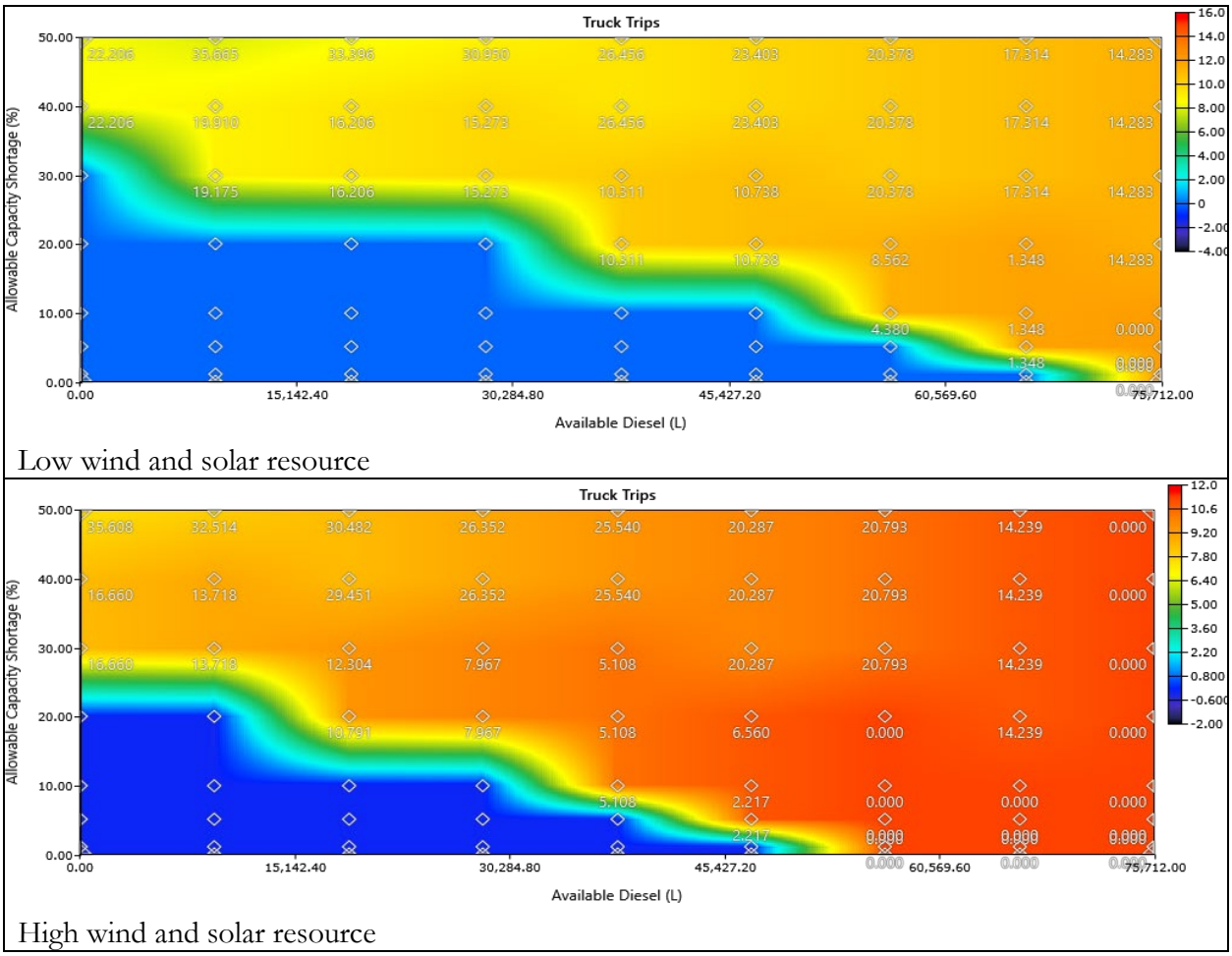

Figure 25. Percent unmet load (diamonds) for various levels of diesel fuel availability for a system architecture consisting of 0 wind systems, 12 PV systems, and 4 battery storage containers

APPENDIX C. CRITICAL LOAD ANALYSIS

The critical load for the base used in this simulation represents 22% of the overall load required to operate the base. Using the different solar and wind resource scenarios (low and high) a 100% renewable system of wind and PV containers plus battery storage can meet the critical load without any diesel fuel, thus providing a resilience value. These "critical-load systems" are presented in Table 22. If these same critical-load systems are deployed along with diesel generators to meet the full regular load of the base with unlimited fuel availability, they will meet between 27% and 35% of the overall base load, thus providing not only a resilience value but also a fuel offset value (Table 23). If the renewable systems are designed from a transportation burden perspective only, and not considering critical loads explicitly, the results are significantly different as shown in Table 24. Most notably, wind systems are not optimally deployed in either of the low wind resource scenarios (row 1 and 3). This contrasts sharply with the wind systems are deployed in both low wind scenarios to meet critical loads (Table 22). This suggests that wind has an inherent resilience value when combined with solar and battery storage that is not obvious when just considering the transportation burden metric.

Table 22. Optimal system architectures to meet critical base loads without diesel

Solar Radiation (kWh/m²/day)	Wind Speed (m/s)	PV (kW)	D3T20	6T	Truck Trips	Ren Frac (%)	Total Fuel (L/yr)	Diesel Generators production (kWh)	PV Production (kWh/yr)	D3T20 Production (kWh/yr)
4.21	4.32	192	2	268	4.3	100	0	0	263,030	72,749
4.21	6.22	64	2	287	3.4	100	0	0	87,677	156,966
5.20	4.32	192	1	299	3.9	100	0	0	329,004	36,374
5.20	6.22	64	2	264	3.3	100	0	0	109,668	156,966

Table 23. Critical load optimized architectures with full load and unlimited diesel fuel

Solar Radiation (kWh/m²/day)	Wind Speed (m/s)	PV (kW)	D3T20	6T	Truck Trips	Ren Frac (%)	Total Fuel (L/yr)	Diesel Generators production (kWh)	PV Production (kWh/yr)	D3T20 Production (kWh/yr)
4.21	4.32	192	2	278	15.0	33	201,751	656,004	263,030	72,749
4.21	6.22	64	2	278	15.3	25	226,117	734,152	87,677	156,966
5.20	4.32	192	1	278	14.1	35	193,917	632,249	329,004	36,374
5.20	6.22	64	2	278	15.0	27	220,586	713,510	109,668	156,966

Table 24. Optimal architectures without constraints on amount of renewables or diesel

Solar Radiation (kWh/m²/day)	Wind Speed (m/s)	PV (kW)	D3T20	6T	Truck Trips	Ren Frac (%)	Total Fuel (L/yr)	Diesel Generators production (kWh)	PV Production (kWh/yr)	D3T20 Production (kWh/yr)
4.21	4.32	640	0	583	12.2	74	77,675	251,206	876,766	0
4.21	6.22	320	7	391	10.6	86	43,368	136,555	438,383	549,380
5.20	4.32	576	0	583	11.0	78	65,309	211,180	987,012	0
5.20	6.22	320	6	418	10.0	87	39,802	124,961	548,340	470,897

DISTRIBUTION

Email—Internal

Name	Org.	Sandia Email Address
Technical Library	01977	sanddocs@sandia.gov

This page left blank

This page left blank

Sandia National Laboratories

Sandia National Laboratories is a multimission laboratory managed and operated by National Technology & Engineering Solutions of Sandia LLC, a wholly owned subsidiary of Honeywell International Inc. for the U.S. Department of Energy's National Nuclear Security Administration under contract DE-NA0003525.